PUBLICATIONS OF
THE UNIVERSITY OF EASTERN FINLAND

Dissertations in Health Sciences

UNIVERSITY OF
EASTERN FINLAND

MEHWISH ANWER

SUSHI REPEAT-CONTAINING PROTEIN X-LINKED 2: A NOVEL HYPOTHALAMO-PITUITARY PROTEIN IN PATHOPHYSIOLOGY OF TRAUMATIC BRAIN INJURY

SUSHI REPEAT-CONTAINING PROTEIN X-LINKED 2: A NOVEL HYPOTHALAMO-PITUITARY PROTEIN IN PATHOPHYSIOLOGY OF TRAUMATIC BRAIN INJURY

Mehwish Anwer

SUSHI REPEAT-CONTAINING PROTEIN X-LINKED 2: A NOVEL HYPOTHALAMO-PITUITARY PROTEIN IN PATHOPHYSIOLOGY OF TRAUMATIC BRAIN INJURY

To be presented by permission of the Faculty of Health Sciences, University of Eastern Finland for public examination in MD100 Auditorium, im Kuopio, on Friday, March 13th 2020, at 12 noon

Publications of the University of Eastern Finland
Dissertations in Health Sciences
No 553

University of Eastern Finland
Kuopio
2020

Series Editors
Professor Tomi Laitinen, M.D., Ph.D.
Institute of Clinical Medicine, Clinical Physiology and Nuclear Medicine
Faculty of Health Sciences

Associate Professor (Tenure Track) Tarja Kvist, Ph.D.
Department of Nursing Science
Faculty of Health Sciences

Professor Kai Kaarniranta, M.D., Ph.D.
Institute of Clinical Medicine, Ophthalmology
Faculty of Health Sciences

Professor Tarja Malm, Ph.D.
A.I. Virtanen Institute for Molecular Sciences
Faculty of Health Sciences

Lecturer Veli-Pekka Ranta, Ph.D.
School of Pharmacy
Faculty of Health Sciences

Distributor:
University of Eastern Finland
Kuopio Campus Library
P.O.Box 1627
FI-70211 Kuopio, Finland
www.uef.fi/kirjasto

Grano Oy, Jyväskylä
2020

ISBN: 978-952-61-3324-9 (print/nid.)
ISBN: 978-952-61-3325-6 (PDF)
ISSNL: 1798-5706
ISSN: 1798-5706
ISSN: 1798-5714 (PDF)

Author's address: A.I. Virtanen Institute for Molecular Sciences
University of Eastern Finland
KUOPIO
FINLAND

Doctoral programme: Doctoral Programme in Molecular Medicine

Supervisors: Professor Asla Pitkanen, MD, Ph.D.
A.I. Virtanen Institute for Molecular Sciences
University of Eastern Finland
KUOPIO
FINLAND

Xavier Ekolle Ndode-Ekane, Ph.D.
A.I. Virtanen Institute for Molecular Sciences
University of Eastern Finland
KUOPIO
FINLAND

Noora Puhakka, Ph.D.
A.I. Virtanen Institute for Molecular Sciences
University of Eastern Finland
KUOPIO
FINLAND

Reviewers: Professor Susanna Narkilahti, Ph.D.
Faculty of Medicine and Health Technology
Tampere University
TAMPERE
FINLAND

Professor Heikki Rauvala, MD, Ph.D.
Helsinki Institute of Life Science
University of Helsinki
HELSINKI
FINLAND

Opponent: Professor Leszek Kaczmarek, Ph.D.
Nencki Institute of Experimental Biology
WARSAW
POLAND

Nothing in life is to be feared, it is only to be understood.
Now is the time to understand more, so that we may fear less.
Marie Curie

Anwer, Mehwish
Sushi repeat-containing protein x-linked 2: A novel hypothalamo-pituitary protein in pathophysiology of traumatic brain injury
Kuopio: University of Eastern Finland
Publications of the University of Eastern Finland
Dissertations in Health Sciences 553. 2020, 78 p.
ISBN: 978-952-61-3324-9 (print)
ISSNL: 1798-5706
ISSN: 1798-5706
ISBN: 978-952-61-3325-6 (PDF)
ISSN: 1798-5714 (PDF)

ABSTRACT

Traumatic brain injury (TBI) refers to a brain injury due to an external mechanical force causing an impact to the head, which leads to the development of neurobiological, psychological, and social abnormalities. Remodelling of the extracellular matrix after TBI is crucial for tissue repair and attenuation of development of co-morbidities including posttraumatic epileptogenesis and endocrine dysfunction. Sushi repeat-containing protein X-linked 2 (SRPX2) is a novel ligand of urokinase-type plasminogen activator receptor (uPAR), which is a key player in the proteolysis of the extracellular matrix and tissue remodeling after TBI. SRPX2 is associated with language development, synaptic plasticity, tissue remodeling and angiogenesis, and mutations in the human *SRPX2* gene have been linked with Rolandic epilepsy and mental retardation. However, the cellular localization of SRPX2 in brain, the SRPX2-uPAR interaction, and the effect of acquired brain injury on SRPX2 expression is unknown.

The aim of this thesis is to study SRPX2 expression in normal rodent, non-human primate and human brain, and its presence in plasma and cerebrospinal fluid. Next, it will be studied whether SRPX2 modulates its effects through its receptor uPAR, and if the deficiency of uPAR or its other ligand, urokinase-type plasminogen activator (uPA), effects SRPX2 expression in brain. Essentially, the study investigates the acute and chronic effects of traumatic brain injury on SRPX2 expression and consequently on the hypothalamo-pituitary axis.

The expression of SRPX2 protein in brain was identified using immunohistochemistry and *in situ* hybridization. The specificity of anti-SRPX2 antibody was confirmed by silencing *SRPX2 in vitro* using siRNA gene silencing technology. *Plaur*$^{-/-}$ and *Plau*$^{-/-}$ mice were used to identify the effect of genetic deficiency of uPAR and uPA on SRPX2 expression. Controlled cortical impact injury (CCI) was induced to examine the effect of traumatic brain injury on SRPX2 expression in wild type, *Plaur*$^{-/-}$ and *Plau*$^{-/-}$ mice. For a comprehensive spatiotemporal profile of SRPX2 protein in brain after TBI, lateral fluid-percussion injury (FPI) model was used in rats, and plasma SRPX2 levels were also quantified using western blot.

Magnetic resonance imaging (MRI) and $MnCl_2$-enhanced MRI (MEMRI) were used to study hypophyseal atrophy after lateral FPI in rats. Seizure susceptibility was assessed using pentylenetetrazol test and spatial learning and memory were evaluated with the Morris water-maze tests.

The results demonstrate that SRPX2 immunoreactive (ir) neurons are present in paraventricular, periventricular, and supraoptic nuclei of mouse, rat, monkey, and human hypothalamus. Dense SRPX2-ir projections from hypothalamic SRPX2-ir positive neurons travel towards the hypophysis terminating in neurohypophysis. SRPX2 protein colocalizes with oxytocin or vasopressin, and SRPX2 is secreted into plasma and CSF in rats and humans. Hypothalamic SRPX2 expression is unaffected by the genetic deficiencies in the urokinase-system or to CCI-induced TBI. However, lateral FPI-induced TBI in rats results in an acute reduction in SRPX2 expression in hypothalamus and plasma. Moreover, a lateral FPI-induced injury in rats leads to a chronic reduction in the neurohypophyseal volume, which relates to increased seizure susceptibility and poor performance in spatial learning tasks.

In conclusion, this study demonstrates that the phylogenetically conserved hypothalamic expression of SRPX2 protein is regulated independent of uPAR, and SRPX2 plasma levels can serve as a biomarker of an acquired brain injury. Furthermore, the lobe-specific hypophyseal volume can be utilized as a prognostic marker of post-TBI outcome.

Keywords: Hypophysis, hypothalamus, lateral fluid-percussion injury, magnetic resonance imaging, manganese-enhanced magnetic resonance imaging, neurohypophysis, oxytocin, paraventricular nucleus, supraoptic nucleus, sushi repeat-containing protein X-Linked 2, traumatic brain injury, urokinase-type plasminogen activator receptor, vasopressin

Anwer, Mehwish
Sushi repeat-containing protein x-linked 2: A novel hypothalamo-pituitary protein in pathophysiology of traumatic brain injury
Kuopio: Itä-Suomen yliopisto
Publications of the University of Eastern Finland
Dissertations in Health Sciences 553. 2020, 78 s.
ISBN: 978-952-61-3324-9 (nid.)
ISSNL: 1798-5706
ISSN: 1798-5706
ISBN: 978-952-61-3325-6 (PDF)
ISSN: 1798-5714 (PDF)

TIIVISTELMÄ

Aivovamman (AV) aiheuttaa ulkoinen päähän kohdistunut mekaaninen voima. Usein AV johtaa neurobiologisiin, psykologisiin ja sosiaalisiin poikkeavuuksiin. Solunulkoinen matriksi on ratkaisevan tärkeä kudoksen toipumiselle ja komorbiditeettien ehkäisylle AV:n jälkeen, ml. post-traumaattinen epilepsia ja endokrinologiset häiriöt. Sushi-repeat containing protein X-linked 2 (SRPX2) on äskettäin löydetty proteiini ja ligandi urokinaasityyppiselle plasminogeeniaktivaattorireseptorille (uPAR), jonka toiminta on välttämätön solunulkoiselle proteolyysille kudosten uudelleenmuokkautuessa. Tähänastiset tutkimukset osoittavat, että SRPX2 osallistuu synaptiseen plastisuuteen, kudosten uudelleenmuotoiluun ja angiogeneesiin, sekä lapsuudenaikaiseen kielelliseen kehitykseen. Ihmisen genetiikkatutkimukset ovat liittäneet SRPX2-geenin mutaatiot Rolandiseen epilepsiaan ja aivojen kehityshäiriöihin. Toistaiseksi meillä ei ole tietoa, missä soluissa SRPX2 ilmenee aivoissa, miten se vuorovaikuttaa uPAR-reseptorinsa kanssa tai miten sen ilmeneminen muuttuu AV:n jälkeen.

Väitöskirjatyössäni tutkin (a) SRPX2:n ilmentymistä jyrsijän ja kädellisten aivoissa ja sen erittymistä plasmaan ja aivo-selkäydinnesteeseen, (b) uPAR järjestelmän geneettisten defektien vaikutusta SRPX2 ilmenemiseen aivoissa, (c) aivovamman vaikutusta SRPX2 ekspressioon, ja (d) plasman SRPX2-tasojen potentiaalia aivovamman biomarkkerina. Tutkimukseni keskittyi SRPX2:n ilmentymiseen akuutissa ja kroonisessa AV:ssä hypothalamus-hypofyysiakselilla.

SRPX2-proteiinin ilmentymisen aivoissa tunnistin immunohistokemiallisesti ja *in situ* -hybridisaatiolla. Vasta-aineen spesifisyyden määritin *in vitro* siRNA-pohjaista SRPX2: n hiljentämistekniikalla. Geneettisten defektien vaikutusta SRPX2 ekpresioon tutkin Plaur$^{-/-}$ ja Plau$^{-/-}$ -hiirillä. AV:n vaikutusta SRPX2:n ilmenemiseen tutkin aivokuoren kontuusiomallissa sekä villityypillä että geneettisesti modifioiduilla hiirillä. SRPX2-proteiinin spatiotemporaalista ilmenemistä eri aivoalueilla AV:n jälkeen tutkin ns. AV:n sekatyyppisessa rottamallissa, jossa harmaan aineen vaurion lisäksi esiintyy valkoisen aineen vauriota. Plasma SRPX2-tasot määritin western blot -menetelmällä. Hypofyysin atrofiaa AV:n jälkeen tutkin rottamallissa

mangaanivahvistetulla magneettikuvantamisella. AV:n jälkeistä kohtauskynnyksen alenemaa tutkin rottamallissa pentyleenitetratsolitestillä ja muistia Morrisin vesisokkelotestillä.

Tulokseni osoittavat, että SRPX2-immunoreaktiiviset (ir) neuronit sijaitsevat hypotalamuksen paravetrikulaarisessa, periventrikulaarisessa ja supraoptisessa tumakkeessa sekä hiiren, rotan, apinan että ihmisen aivoissa. Hypotalamisten SRPX2-ir-positiivisten hermosolujen viejähaarakkeet eli aksonit kulkevat kohti hypotalamuksen ventraaliosia ja sieltä kaudaalisesti päätyen hypofyysin posterioriseen osaan eli neurohypofyysiin. Hypotalamuksessa SRPX2-proteiini sijaitsee samoissa hermosoluissa kuin oksitosiini ja vasopressiini. SRPX2 löytyy plasmasta sekä rotalla että ihmisellä. SRPX2:n ilmentyminen hypotalamuksessa on resistentti urokinaasijärjestelmän geneettisille mutaatioille. Myöskään aivokontuusiomallissa hiirellä SRPX2:n ekspressiossa ei tapahtunut suurempaa muutosta. Ns. suljetun aivovamman rottamallissa SRPX2:n ilmentyminen vähentyi merkittävästi hypotalamuksessa, mikä assosioitui alhaisiin SRPX2-plasmapitoisuuksiin. Kyseisessä rottamallissa havaitsin myös merkittävän hypofyysin tilavuuden pienenemisen. Rotilla oli myös alentunut kohtauskynnys ja heikentynyt avaruudellinen oppiminen.

Yhteenvetona totean, että tutkimukseni perusteella SRPX2-proteiini on fylogeneettisesti konservoitunut hypotalamukseen, eikä sen ilmeneminen riipu uPAR-reseptorin ekspressiosta. Käytetyssä rottamallissa alhainen SRPX2-plasmataso näyttäisi toimivan biomarkkerina aivovammalle. Lisäksi hypofyysin posteriorisen osan tilavuus näyttäisi ennustavan kyseisessä eläinmallissa AV:n pitkäaikaisennustetta.

Avainsanat: Hypofyysi, hypotalamus, magneettiresonanssikuvaus, mangaanivahvistettu magneettikuvaus, neurohypofyysi, oksitosiini, paraventrikulaarinen ydin, supraoptinen ydin, sushi-repeat containing protein X-Linked 2, traumaattinen aivovaurio, urokinaasityyppinen plasminogeeniaktivaattori, vasopressiini

ACKNOWLEDGEMENTS

This study was carried out at the A. I. Virtanen Institute for Molecular Sciences, University of Eastern Finland during the years 2015-2019.

I am grateful to my supervisor, Professor Asla Pitkanen, MD, PhD, for her support and supervision duing this PhD. Her inquisitive approach to research has inspired me to think critically and analytically. I am thankful to my co-supervisors, Xavier Ekolle Ndode-Ekane, PhD, and Noora Puhakka, PhD, for their contribution and support in completion of this thesis. I am indebted to Professor Eleonora Aronica for her supervision and guidance during my secondment in her lab.

I am thankful to my co-authors Nea Bister, Stina Leskela, Dr Tamuna Bolkvadze, Dr Thomas Rauramaa, Dr Ville Leinonen, Dr Erwin van Vliet, Dr Riikka Immonen, Dr Nick Hayward, Dr Leonardo Lara Valderrabano, Dr Jenni Karttunen, Dr Haapasalo Annakaisa, Professor Tarja Malm, Professor Olli Grohn, Professor Synnove Carlson, Professor Dick Swaab and Professor Eleonora Aronica for their contribution to the research presented in this thesis.

I am thankful to the entire "Epiclub" for their company and interesting journal club sessions. Special thanks to Ms Merja Lukkari and Mr Jarmo Hartikainen for their technical assistance and generous support. I am thankful to UEF-AIVI personnel, especially Joanna Huttunen, Asta Suhonen, Jussi Keinanen, Hanne Tanskanen, Marja Jarvelainen and Jari Nissinen, for their everlasting help in solving the never-ending adminstrative issues for an international student.

A special thank you to my beloved, Atif, for his unconditional love and empowering presence in my life. The warmth and radiance of your love helped me survive the long polar nights. You always believed in me, even when I doubted myself. I appreciate this more than you know. Finally, I would like to thank my family for their love and support throughout my life.

This project was supported by the European Union's Horizon 2020 research and innovation programme under the Marie Sklodowska-Curie grant agreement N° 642881 ECMED, The Finnish Epilepsy Research Foundation, The Finnish Brain Foundation, The Maire Taposen Foundation and The University of Eastern Finland.

Mehwish Anwer
Kuopio, September 2019

LIST OF ORIGINAL PUBLICATIONS

This dissertation is based on the following original publications that are referred to by their roman numerals:

I Anwer M, Bolkvadze T, Ndode-Ekane XE, Puhakka N, Rauramaa T, Leinonen V, van Vliet EA, Swaab DF, Haapasalo A, Leskela S, Bister N, Malm T, Carlson S, Aronica E, Pitkänen A. Sushi repeat-containing protein X-Linked 2 - a novel phylogenetically conserved hypothalamo-pituitary protein. Journal of Comparative Neurology, 526:1806–1819, 2018.

II Anwer M, Bolkvadze T, Puhakka N, Ndode-Ekane XE, Pitkänen A. Genotype and injury effect on the expression of a novel hypothalamic protein sushi repeat-containing protein X-linked 2 (SRPX2). Neuroscience, 415:184-200, 2019.

III Anwer M, Valderrabano LL, Karttunen J, Ndode-Ekane XE, Puhakka N, Pitkänen A. Acute downregulation of novel hypothalamic protein sushi repeat-containing protein X-linked 2 (SRPX2) after experimental traumatic brain injury. Journal of Neurotrauma, 2019, In press.

IV Anwer M, Immonen R, Hayward MEAN, Ndode-Ekane XE, Puhakka N, Gröhn O, Pitkänen A. Lateral fluid-percussion injury leads to pituitary atrophy in rats. Scientific Reports, 9(1):11819, 2019.

The publications were adapted with the permission of the copyright owners.

''It is and will remain a wound which I live above but which is there deep down and cannot heal - years from now it will be what it was the first day.''
Vincent van Gogh on trauma

CONTENTS

ABSTRACT **7**

TIIVISTELMÄ **9**

ACKNOWLEDGEMENTS **11**

LIST OF ORIGINAL PUBLICATIONS **13**

CONTENTS **15**

ABBREVIATIONS **17**

1 INTRODUCTION **19**

2 REVIEW OF THE LITERATURE **21**
2.1 Traumatic Brain Injury 21
2.1.1 Current state of clinical management of TBI 22
2.1.2 Biomakers of TBI 22
2.2 Experimental models of TBI 23
2.2.1 Controlled cortical impact injury (CCI) 23
2.2.2 Lateral fluid-percussion injury (Lateral FPI) 24
2.3 Hypothalamo-pituitary axis in TBI 24
2.3.1 Hypophysis and Magnetic Resonance Imaging 25
2.4 Extracellular matrix of the brain 27
2.4.1 Extracellular matrix remodelling and the uPAR interactome 27
2.5 Sushi repeat-containing protein X-linked 2 28
2.5.1 SRPX2 and uPAR 28

3 AIMS OF THE STUDY **31**

4 SUBJECTS AND METHODS **33**
4.1 Overview 34
4.2 Subjects and animals 34
4.2.1 Humans (I) 35
4.2.2 Monkeys (I) 35
4.2.3 Rats (I, II, IV) 35
4.2.4 Mice (I-II) 35
4.3 Experimental models of TBI 36
4.3.1 Induction of controlled cortical impact injury (II) 36
4.3.2 Induction of lateral fluid-percussion injury (III-IV) 36
4.4 Processing of tissue for histology 37
4.4.1 Humans (I) 37
4.4.2 Monkeys (I) 37
4.4.3 Rats and mice (I-III) 37
4.5 Antibody specificity (I) 38
4.6 *In situ* hybridization (I) 40
4.7 Immunohistochemistry (I-III) 40
4.7.1 SRPX2 and oxytocin immunohistochemistry (I-III) 40
4.7.2 Quantitative analysis (I-III) 41

4.8 Immunofluorescence (I) 41
4.9 Nissl Staining (I-III) 42
4.10 Plasma and cerebrospinal fluid samples (I, III) 43
4.11 Western blot (I, III) 43
4.12 Magnetic Resonance Imaging (IV) 44
4.13 $MnCl_2$-enhanced MRI (MEMRI) (IV) 44
4.14 Pentylenetetrazol test (IV) 45
4.15 Morris water-Maze Test (IV) 45
4.16 Statistical analysis (I-IV) 45
4.16.1 Unsupervised hierarchial clustering analysis (II-III) 46

5 RESULTS 47
5.1 Specificity of SRPX2 antibody (I) 47
5.2 SRPX2 is expressed in normal brain (I) 47
5.3 Hypothalamic SRPX2 expression is highly conserved and can be detected in plasma (I) 48
5.4 SRPX2 expression is regulated independent of uPAR (II) 49
5.5 hypothalamic SRPX2 expression remains unaltered after CCI-induced TBI in mice (II) 49
5.6 CCI differentially regulates uPAR and uPA gene expression in mice (II) 50
5.7 SRPX2 expression is downregulated acutely after FPI (III) 51
5.7.1 SRPX2 expression in plasma after lateral FPI (III) 51
5.7.2 Hypothalamic SRPX2-ir neurons after lateral FPI (III) 52
5.7.3 FPI-induced SRPX2 expression in plasma correlates with brain (III) 53
5.7.4 Hypothalamic oxytocin-ir neurons after lateral FPI (III) 53
5.8 Lateral FPI leads to reduction in neurohypophyseal volume (IV) 54
5.9 Neurohypophyseal volume correlates with seizure susceptibility and impaired spatial learning (IV) 55
5.10 Summary of results 55

6 DISCUSSION 57
6.1 Methodological considerations 57
6.1.1 Human brain tissue 57
6.1.2 Animal models 57
6.1.3 Gender effect 58
6.1.4 RNA analysis 58
6.1.5 Immunological methods 58
6.1.6 Western blot 59
6.2 SRPX2 expression in normal brain 59
6.3 SRPX2 and the uPAR interactome 61
6.4 SRPX2 expression after traumatic brain injury 62
6.5 SRPX2 as a biomarker of Hypothalamic injury after TBI 63
6.6 Hypothalamo-pituitary axis in TBI 64

7 CONCLUSIONS 67

REFERENCES 69

APPENDICES 79

ORIGINAL PUBLICATIONS (I – IV) 81

ABBREVIATIONS

AUC	Area under the curve
BCIP	5-bromo-4-chloro-30-indolyphosphate p-toluidine salt
CCI	Controlled cortical impact injury
CSF	Cerebrospinal fluid
DMSO	Dimethylsulfoxide
ECM	Extracellular matrix
ELISA	Enzyme-linked immunosorbent assay
ESCC	Tissue esophageal squamous cell carcinoma
FPI	Fluid-percussion injury
GBM	Glioblastoma
GCS	Glasgow coma scale
HCC	Hepatocellular carcinoma
HPA	Hypothalamo-pituitary-adrenal axis
HRP	Horseradish peroxidase
IF	Immunofluorescence
IHC	Immunohistochemistry
ISH	*In situ* hybridization
KPBS	Potassium phosphate buffered saline
MEMRI	$MnCl_2$-enhanced MRI
MGE	Multi echo gradient echo
MRI	Magnetic resonance imaging
MWM	Morrise water-maze
NBT	Nitro-blue tetrazolium chloride
NGS	Normal goat serum
Pa	Paraventricular nucleus
PaAP	Anterior parvocellular Pa
PaDC	Dorsal cap Pa
PAI	Plasminogen activator inhibitors
PaLM	Lateral magnocellular Pa
PaMM	Medial magnocellular Pa
PaMP	Medial parvocellular Pa
PaPO	Posterior Pa
PaV	Ventral part of Pa

PDAC Pancreatic ductal adenocarcinoma

Pe Periventricular nucleus

PFA Paraformaldehyde

PTSD Post-traumatic stress disorder

PTZ 1,5-pentamethylenetetrazole

ROI Region of interest

RT Room temperature

RT-qPCR Reverse transcriptase-quantitative polymerase chain reaction

SDS-PAGE SDS-polyacrylamide gel electrophoresis

siRNA Small interfering RNA

SO Supraoptic nucleus

SRPX2 Sushi repeat-containing protein X-linked 2

TBI Traumatic brain injury

uPA Urokinase-type plasminogen activator

uPAR Urokinase-type plasminogen activator receptor

WB Western blot

Wt Wild type

1 INTRODUCTION

Globally, an estimated 69 million people sustain traumatic brain injury (TBI) each year and suffer from neurobiological, psychological and social consequences of the injury (Dewan et al., 2018). TBI results in 15-20% of all cases of acquired epilepsy and 5% of all type of epilepsies (Herman, 2002; Klein et al., 2017). In addition to neurological and systemic changes, TBI causes long-term neuroendocrine dysregulation in up to 40% of humans due to functional damage to the hypothalamic-pituitary axis (Dusick et al., 2012; Gasco et al., 2012; Richmond and Rogol, 2014; Guaraldi et al., 2015). TBI leads to tissue damage, hemorrhages, impaired metabolism and gene expression, and hence the development of neurological comorbidities (Maas et al., 2008). Therefore, post-injury remodeling of the extracellular matrix is crucial for tissue recovery and the mitigation of development of co-morbidities including posttraumatic epileptogenesis (Soleman et al., 2013; Pitkänen and Immonen, 2014).

Urokinase-type plasminogen activator receptor (uPAR), a key player in the fibrinolytic system, modulates processes like cellular proliferation, adhesion and migration through proteolysis of the extracellular matrix (ECM) (Sumi et al., 1992; Preissner et al., 2000; Semina et al., 2016). The uPAR interactome consists of uPAR and its ligands, including urokinase-type plasminogen activator (uPA) and sushi repeat-containing protein X-linked 2 (SRPX2), tissue-type plasminogen activator (tPA) and plasminogen activator inhibitors (PAI-1, PAI-2) (Eden et al., 2011).

Sushi repeat-containing protein X-linked 2 (SRPX2) is a novel ligand of uPAR. SRPX2 has been shown to modulate language development, angiogenesis, synaptic plasticity, and tissue remodeling (Roll et al., 2006, 2010; Royer-Zemmour et al., 2008a; Sia et al., 2013). Mutations in human *SRPX2* gene have been associated with Rolandic epilepsy, speech dyspraxia and mental retardation (Roll et al., 2006, 2010). The coinciding physiological roles of SRPX2 and uPAR, and the SRPX2-uPAR interaction indicate SRPX2 as a candidate target for tissue remodeling and repair after TBI. However, the precise localization of SRPX2 in the brain, the interaction of SRPX2 with uPAR and the effect of acquired brain injury of SRPX2 expression are unknown.

The aim of this thesis is to, first, characterize the expression of SRPX2 protein in normal rodent, non-human primate and human brain, to identify cell type-specific expression of SRPX2 protein, and to investigate if it is secreted to plasma or cerebrospinal fluid. Secondly, to elucidate whether SRPX2 expression is modulated by the uPAR interactome, and if the deficiency of uPAR or its other ligand, urokinase-type plasminogen activator (uPA), effects the expression of SRPX2 in brain. Next, the study focuses, particularly, on deciphering the effects of an acquired brain injury on the expression of SRPX2 protein in brain and plasma, and whether the plasma SRPX2 levels can serve as a biomarker of TBI. In view of SRPX2 expression in hypothalamo-pituitary

axis, it was also investigated whether experimental TBI leads to hypophyseal atrophy, and if it associates with seizure susceptibility and memory performance.

2 REVIEW OF THE LITERATURE

2.1 TRAUMATIC BRAIN INJURY

Traumatic brain injury is an increasing health and economic burden. Globally, about 69 million people live with TBI leading to morbidity and mortality (Dewan et al., 2018). The main causes of TBI include, but are not limited to, falls, car accidents, sports activities and military activities. The incidence of TBI is increasing in low-income and middle-income countries due to traffic incidents whereas in high income countries TBI incidence is increasing in elderly patients mainly due to falls. For instance, traffic incidents are the leading cause of TBI (54%) in China, followed by falls (32–33%) and violence (9–11%) (Maas et al., 2017). In addition to TBI-induced pathology, TBI also serves as a risk factor for development of neurodegenerative diseases like epilepsy and stroke. Traumatic brain injury (TBI) causes 15-20% of all acquired epilepsies (Klein et al., 2017; Andrade et al., 2018). In addition to post-TBI neurological changes, about 25-40% of TBI patients develop chronic hypopituitarism (Dusick et al., 2012; Gasco et al., 2012; Richmond and Rogol, 2014; Guaraldi et al., 2015) due to alterations in the neuroendocrine system (Kasturi and Stein, 2009). Not only does severe TBI exhibit a high mortality rate, it also poses a substantial physical, psychiatric, emotional and economic burden (Rosenfeld et al., 2012).

Rehabilitation is essential for the individuals who sustain a brain injury. This is because TBI greatly affects the lives of the survivors and their families, and consequently increase burden of physical, psychiatric, emotional and cognitive disabilities. These long-term impairments lead to difficulties in daily life activities, work, social life and relationships. Rehabilitation interventions constitute strategies that focus on re-establishing previously learned behavioural patterns (e.g. attention), substitute impaired functions (e.g. assistive technologies for memory impairment) and accommodate residual impairments through cognitive reconstruction for positive psychosocial adjustment (Maas et al., 2017).

According to the definition provided by National Institute of Neurological Disorders and Stroke (NINDS), TBI is defined as "An alteration in brain function, or other evidence of brain pathology, caused by an external force" (Maas et al., 2017). TBI can differ in severity and TBI patients are categorized based on severity using the Glasgow Coma Scale (GCS scale) which provides a score calculated using visual, motor and verbal responses of the patient. Therefore, TBI can be mild (GCS 13–15), moderate (GCS 9–12) or severe (GCS 3–8) (Teasdale and Jennett, 1974). TBI induced damage can be generally classified into primary and secondary injury. Primary injury refers to the damage caused by the mechanical forces at the time of injury including hemorrhage, diffuse axonal injury, cellular injury and necrosis. Secondary injury refers to myriad of events that happen in response to the primary injury, and not due to the external forces as such.

They may include, but are not limited to, ischemia, edema, inflammation, and neuronal cell loss resulting in compromised neuroplasticity, neurocognitive dysfunction and hypothalamic-pituitary dysfunction. While the primary injury lasts between seconds to minutes after injury, the secondary injury continues from minutes to years after the initial insult explaining, the evolution of associated pathologies and co-morbidities (Reifschneider et al., 2015).

2.1.1 Current state of clinical management of TBI

Currently, the clinical management of TBI utilzes both medical and surgical interventions. For instance, in the intensive care unit, TBI management includes the prevention of secondary insults like hypoxia, hypotension, optimization of cardiorespiratory physiology, control of intracranial pressure and the maintenance of cerebral perfusion pressure (Rosenfeld et al., 2012; Algattas and Huang, 2013; Maas et al., 2017). However, a detailed characterization of the injury type and severity is needed to classify TBI patients. Conventionally, the severity of TBI is classified using the Glasgow coma scale (GCS scale), which evaluates the level of consciousness in patients after the TBI but does not account for mechanistic heterogeneity of TBI (Teasdale and Jennett, 1974). Therefore, the improvement in the characterization of TBI-induced damage relies on the discovery of blood-based, genomic and neuroimaging biomarkers.

2.1.2 Biomakers of TBI

According to the BEST Resource (Biomarkers, EndpointS, and other Tools Resource, 2016) developed by the FDA-NIH Biomarker Working Group, a biomarker can be defined as "A characteristic that can be objectively measured and evaluated as an indicator of normal biological processes, pathogenic processes, or biological responses to a therapeutic intervention". There is an unmet need for development of robust biomarkers, adjunct to neuroimaging, to facilitate diagnosis, prognosis and improvement of TBI-induced outcome. Rapid dynamic changes occur after TBI, which result in time course dependent alterations in the concentrations of biomarkers. Based on the current knowledge of biomarkers of injury, the progressive nature of TBI pathology can be outlined into three general phases; acute (minutes to hours), sub-acute (days) and chronic (weeks to months to years) (Algattas and Huang, 2013; Moghieb and Northwest, 2015; Maas et al., 2017). The acute phase biomarkers of injury to central nervous system consist of following markers; (a) cellular injury (UCH-L1, NSE), (b) neurite degeneration (SBDP/MAP2, c-Tau, NF-H) and (c) gliosis (GFAP, BDP, S100b) (Moghieb and Northwest, 2015). The recent Scandinavian Neurotrauma Committee guidelines recommend use of blood biomarker S100B to stratify patients for CT imaging in acute post-TBI phase (Undén et al., 2015). Neurofilament (NF-H) has been used to track disease progression during the sub-acute phase of injury in rodents. However, it is still to be validated in patients (Undén et al., 2015). Chronic post-traumatic outcomes

are difficult to predict because of the variable time of onset, even when specific types of insults occur. Therefore, investigations focused on temporal profiling of posttraumatic molecular and cellular changes can significantly add to the current knowledge of diagnostic biomarkers for TBI.

2.2 EXPERIMENTAL MODELS OF TBI

TBI is a complex disease and exhibits pathophysiological heterogeneity in the evolution of secondary injury outcome and comorbidities. Various animal models of TBI replicate the distinct features of human TBI and facilitate the identification of underlying pathological processes. Most TBI studies use adult male rodents because of two main reasons; firstly, TBI is more prevalent in male patients, and secondly, to avoid potential influence of female hormones on TBI outcomes (Wei and Xiao, 2013). The most widely used and highly reproducible animal models of TBI include fluid-percussion injury (FPI) and controlled cortical impact (CCI) injury (Xiong et al., 2013).

2.2.1 Controlled cortical impact injury (CCI)

CCI is a widely used experimental model of the closed-head injury in humans including concussion, diffuse axonal injury and intracranial hematoma commonly caused due to sports activites, car accidents and falls (Wei and Xiao, 2013). CCI utilizes an impact device to deliver a force onto the exposed but intact dura using a pneumatically driven pistol. It mimics human TBI and results in a concussion, cortical damage, subdural heamatoma and dysfunctional blood-brain barrier (Statler et al., 2008; Statler et al., 2009; Hunt et al., 2009; Hunt et al., 2010; Hunt et al., 2011; Bolkvadze and Pitkänen, 2012; Hunt et al., 2012). In comparison to other TBI models, CCI offers control on mechanical factors including time, velocity and depth of impact and is therefore more useful in mechanistic studies (Xiong et al., 2013). CCI leads to a focal cortical injury resulting in extensive damage to the gray and white matter (Pitkänen and Immonen, 2014; Drexel et al., 2015). Numerous studies have characterized the neuropathological hallmarks of CCI and identified widespread damage to cortex, hippocampus and thalamus (Bolkvadze and Pitkänen, 2012a). Furthermore, mice subjected to CCI-induced injury exhibited increased vasopressin synthesis in hypothalamus and perilesional cortex (Szmydynger-Chodobska et al., 2011). CCI recaputulates human TBI by exhibiting functional deficits including impaired learning, memory, motor function and overall neurological function as assessed by behavioural tests like Morris water maze test, elevated plus maze, neuroscore, beam walking task etc (Osier and Dixon, 2016). Furthermore, studies in mice with CCI demonstrated increased susceptibility to PTZ-induced seizures and the occurrence of electrographic spontaneous seizures (Bolkvadze and Pitkänen, 2012b)

2.2.2 Lateral fluid-percussion injury (Lateral FPI)

In the fluid-percussion model of injury (FPI), an impact is produced onto the exposed yet intact dura by a fluid pressure pulse generated by striking a fluid filled reservoir mimicing coup-contrecoup injury in humans. Depending on the site of the craniotomy, FPI can be mid-line or lateral producing both focal and diffuse brain injury (Xiong et al., 2013). The lateral FPI is the most commonly used animal model of TBI in rats. FPI replicates the clinical TBI without causing a skull fracture including brain swelling, intracranial hemorrhage, and grey matter damage. Lateral FPI results in a focal contusion and a diffused subcortical injury, including acute and chronic damage to the hippocampus, thalamus and hypothalamus (Thompson et al., 2005b). Lateral FPI also recapitulates several neurobehavioral, sensorimotor, neuromotor and cognitive deficits observed in humans after TBI. For instance, long-term impaired coordination in movement and posture are commonly observed in humans after TBI. Rats with lateral FPI exhibited similar deficits when assessed with composite neuroscore (Thompson et al., 2005b). Furthermore, 30-50% of rats that receive a lateral FPI develop spontaneous seizures, providing an opportunity to investigate mechanisms underlying posttraumatic epilepsy (Kharatishvili et al., 2006; Kharatishvili and Pitkanen, 2010).

None of the currently available TBI models are exhaustive in modelling human TBI. However, both CCI and lateral FPI are widely used to study pathological changes caused by TBI as they provide insights into various aspects of human TBI. For instance, CCI provides more flexibility in scaling down injury to smaller rodents compared to FPI (Osier and Dixon, 2016). Moreover, CCI has a low mortality rate relative to FPI. However, CCI presents a focal contusion and localized cortical damage but lateral FPI results in a more diffused injury and affects sub-cortical regions as well (Peterson et al., 2015). Therefore, both CCI and FPI were used in this study to identify cortical and sub-cortical impact of TBI and resultant changes in protein expression.

2.3 HYPOTHALAMO-PITUITARY AXIS IN TBI

The hypothalamus is a complex structure, situated at the base of the brain, connected ventrally to the hypophysis (also known as the pituitary gland). The hypothalamo-pituitary axis controls neuroendocrine and autonomic functions to maintain homeostasis (Swanson and Sawchenko, 1983). The cytoarchitectural organization of hypothalamus comprises of major cell groups and fiber pathways including the paraventricular (Pa) and supraoptic nuclei (SO) and their projections. The neurons of the Pa and SO nuclei synthesize oxytocin and vasopressin, and send axonal projections to the neurohypophysis (Swanson and Sawchenko, 1983). The hypophysis is comprised of two anatomicaly and functionally distinct lobes, namely adenohypophysis (anterior lobe) and the neurohypophysis (posterior lobe) (Dorton, 2000).

Damage to the hypothalamo-pituitary axis can result in chronic hypothalamic and pituitary dysfunction (Tanriverdi et al., 2015). For example, hypopituitarism is prevalent in 11-69% of adults after TBI (Gasco et al., 2012; Richmond and Rogol, 2014; Guaraldi et al., 2015) and is defined as the inability of the pituitary gland to produce physiologically adequate hormones. Hypopituitarism may result in growth hormone deficiency, corticotroph deficiency, thyrotropin deficiency, gonadotropin deficiency, prolactin deficiency and anti-diuretic hormone deficiency. Clinical signs and symptoms of hypopituitarism include fatigue, hypotension, hypoglycaemia, weight disturbances, polyuria, decreased muscle and bone mass, to name a few (Kim, 2015). Moreover, numerous studies have reported abnormalities in the hypothalamo-pituitary-adrenal (HPA) axis after a TBI (Grundy et al., 2001) (see table 1). The TBI-induced dysregulation of vasopressin results in impaired water balance in the body and consequently diabetes insipidus (Capatina et al., 2015). The anatomical similarities between the hypothalamo-pituitary axis of rodents and humans facilitates the identification of TBI-induced damage in experimental TBI models, and provides an opportunity to identify novel modulators of post-TBI outcome.

Chronic hypopituitarism and TBI both result in neurobehavioural deficits including depression, fatigue, anxiety and impaired memory (Pitkänen et al., 2014a; Booij et al., 2018). Untreated TBI-induced endocrinopathy may lead to a post-traumatic stress disorder (PTSD) (Yehuda, 2001). Abnormalities in the HPA axis have been also reported in human cases of temporal lobe epilepsy (Wulsin et al., 2016). However, the role of HPA axis dysfunction in the generation of seizures and TBI-induced comorbidities is still unknown.

2.3.1 Hypophysis and Magnetic Resonance Imaging

The hypophysis is located in the sella turcica and is attached to the hypothalamus through the median eminence. This anatomical organization of hypophysis at the base of the skull is highly similar between rats and humans (Dusick et al., 2012; Tanriverdi et al., 2015). Therefore, neuroimaging studies in experimental models of TBI investigating the alterations in the hypothalamo-pituitary axis provide a good opportunity to identify biomarkers of TBI and its associated abnormalities.

Magnetic resonance imaging (MRI) is a multipurpose non-invasive method that can be used to image brain and hypophysis, and allows the study of disease progression after an insult to the brain (Makulski et al., 2008). MRI has been used previously to identify infarction and hemorrhagic lesions in human hypophysis (Makulski et al., 2008). Another MRI based retrospective study in patients with TBI identified an acute increase in hypophyseal volume which normalized within 8-15 months of the injury (Maiya et al., 2008). However, very few studies have exploited MRI to investigate hypophyseal atrophy in rodents after experimental TBI (Kasturi and Stein, 2009; Greco et al., 2013; Russell et al., 2018).

Manganese-enhanced MRI (MEMRI) is a modification of MRI where Mn^{2+} based contrast enhancement is utilized to study areas of brain without a blood-brain barrier. For instance, systemic administration of $MnCl_2$ allows distinct visualization of both hypophyseal lobes (Silva et al., 2004). MEMRI has been employed to study the anatomy and functional circuits of rodent brain *in vivo* (Aoki et al., 2004). A recent study utilized Teslascan, an FDA approved chelated manganese-based contrast agent, for MEMRI scan of brain and pituitary gland in healthy adult volunteers. However, the method needs further evaluation and assessment before it can be potentially used for neuroradiological investigations (Kim, 2015).

Table 1. Studies describing changes in the hypothalamo-pituitary axis in experimental TBI models. All studies were conducted in male rats. Abbreviations: CCI, Controlled cortical impact; CRH, corticotropin-releasing hormone; FPI, fluid-percussion injury, Pa, paraventricular nucleus; SD, Sprague Dawley.

Animal	Injury model	Sample type	Post-TBI follow-up time	Finding	Reference
Rats, SD	Lateral FPI	Brain tissue	1 h	Bilateral acute hemorrhage in hypothalamus	(Yuan and Wade, 1991)
Rats, SD	Lateral FPI	Brain tissue	2 h	↑ *CRH* mRNA expression in hypothalamic Pa nucleus	(Roe et al., 1998)
Rats, Wistar	Lateral FPI	Brain tissue	2 h and 4 h	↑ *CRH* mRNA expression in hypothalamic Pa nucleus	(Grundy et al., 2001)
Rats, SD	Lateral FPI	Brain tissue	7 d	Hypothermia associated with number of IL-1b+/ED-1+ microglia in hypothalamic Pa nucleus	(Thompson et al., 2005a)
Rats, SD	CCI	Brain tissue, blood, hypophysis	2 months	↓ GH in serum and adenohypophysis, ↑IL-1β in hypothalamus, ↑GFAP in hypothalamus and adenohypophysis	(Kasturi and Stein, 2009)
Rats, SD	Lateral FPI	Brain tissue	1 month	Disruption in sleep-wake behavior, ↓ number of orexin-A+ neurons in lateral hypothalamus	(Skopin et al., 2015)

2.4 EXTRACELLULAR MATRIX OF THE BRAIN

The extracellular matrix (ECM) of the brain consititutes the microenvironment in which neurons and glial cells exit. Essentialy, ECM provides structural support and facilitates intercellular communication. The ECM undergoes changes during the development of the central nervous system (CNS) and supports neurogenesis, synaptogenesis, gliogenesis, cellular migration and axonal outgrowth during adulthood. ECM is primarily composed of proteoglycans which constitute the macromolecular structure on the surface of neurons called perineuronal nets (PNNs) (Soleman et al., 2013). Other ECM components include hyaluronan, aggrecan, brevican, fibronectin, tenascin and laminin amongst others. ECM components are degraded by special extracellular proteolytic enzymes called matrix metalloproteinases (MMPs). The fibrinolytic system of the ECM is regulated through the Urokinase-type plasminogen activator receptor (uPAR) interactome (Sumi et al., 1992; Preissner et al., 2000; Semina et al., 2016). The ECM molecules play a central role in pathogenesis of CNS diseases like spinal cord injury, stroke and TBI (Soleman et al., 2013).

2.4.1 Extracellular matrix remodelling and the uPAR interactome

The. In the adult brain, ECM affects cell survival, plasticity, damage responses and regeneration (Soleman et al., 2013). TBI evokes a pathological remodeling of ECM of the brain, and in some cases, the development of tissue capable of generating seizures (epileptogenesis) (Pitkänen et al., 2014b). Therefore, it is important to identify post-traumatic molecular and cellular changes in the components of ECM underlying the development of the posttraumatic outcome, including posttraumatic epilepsy.

Urokinase-type plasminogen activator receptor (uPAR) is a key component in the ECM fibrinolytic system (Sumi et al., 1992; Preissner et al., 2000; Semina et al., 2016). The uPAR interactome consists of uPAR and its ligands, including urokinase-type plasminogen activator (uPA), tissue-type plasminogen activator (tPA) and plasminogen activator inhibitors (PAI-1, PAI-2) (Eden et al., 2011). Alterations in the components of the uPAR interactome have been identified in experimental models and human epilepsy (Masos and Miskin, 1997; Lahtinen et al., 2006a, 2009; Royer-Zemmour et al., 2008a; Iyer et al., 2010; Liu et al., 2010; Bruneau and Szepetowski, 2011; Quirico-Santos et al., 2013; Rantala et al., 2015). uPAR (encoded by *Plaur* gene) and uPA (encoded by *Plau* gene) deficient mice have been used to study the functions of the uPAR interactome in pathological conditions (Bugge et al., 1995; Bolkvadze et al., 2016). The Plaur-deficient mice (*Plaur*$^{-/-}$) develop normally and are fertile in adulthood (Bugge et al., 1995). Previous studies have reported that Plaur-deficient mice exhibit higher chemically induced seizure susceptibility and increased anxiety (Powell et al., 2003).Furthermore, *Plaur*-deficiency in mice leads to aberrant cortical development and impaired hippocampal circuitries (Powell et al., 2003). Moreover, a severe epilepsy phenotype and an impaired inflammatory response was observed in *Plaur*-deficient mice after an

intrahippocampal kainite injection (Ndode-Ekane and Pitkänen, 2013). The Plau-deficient (*Plau*$^{-/-}$) mice also develop normally and do not show any physiological abnormalities (Carmeliet et al., 1993). In *Plau*-deficient mice, tissue repair and motor recovery were impaired after TBI (Lahtinen et al., 2006b, 2009; Bolkvadze et al., 2015). Overall, the uPAR interactome has an important role in post-TBI outcome but the contributing mechanisms are yet to be elucidated.

Sushi repeat-containing protein X-linked 2 (SRPX2) is a novel ligand of uPAR and has been associated with Rolandic epilepsy (Royer-Zemmour et al., 2008a). However, the contribution of uPAR interactome in regulation of SRPX2 is still unclear.

2.5 SUSHI REPEAT-CONTAINING PROTEIN X-LINKED 2

SRPX2 was first recognized as a downstream molecule of E2A-HLF fusion gene in t(17;19)-positive leukemia cells (Kurosawa et al., 1999). Later, a whole genome mutation screen analysis in human patients with Rolandic epilepsy identified pathologic mutations in *SRPX2* gene (Y722S or N327S) which were linked with bilateral perisylvian polymicrogyria, mental retardation and speech dyspraxia (Roll et al., 2006). However, the role of the mutated *SRPX2* gene in epilepsy is debatable because the patients also had a mutation in the *GRIN2A* gene (Lesca et al., 2013).

SRPX2, initially known as SRPUL, is a 465-amino acid protein with a calculated molecular mass of 53 kDa. SRPX2 has an N-terminal signal peptide and 3 consensus sushi repeats, spanning about 60 amino acids each and it contains 6 conserved cysteines (Royer et al., 2007). SRPX2 expression was reported in language cortex, and *in utero* silencing of *Srpx2* resulted in impaired ultrasound vocalizations and epileptiform activity in mice (Roll et al., 2006; Sia et al., 2013). SRPX2 is a secreted protein and its expression was also associated with angiogenesis and the facilitation of adhesion of cancer cells. Tissue SRPX2 levels were identified as a marker of poor prognosis in hepatocellular carcinoma patients (Lin et al., 2017). An overview of studies describing the expression and role of SRPX2 in different human diseases is given in table 2. Despite the distinct effects of SRPX2 on language, angiogenesis, cellular adhesion and synaptic plasticity, there are no reports of the cellular localisation and spatial distribution of SRPX2 in brain.

2.5.1 SRPX2 and uPAR

The interaction of the SRPX2 protein with extracellular proteolytic proteins like urokinase-type plasminogen activator receptor (UPAR), cathepsin B (CTSB), and aggrecanase-1 (ADAMTS4) was identified using a yeast 2-hybrid analysis of human brain cDNA library (Royer-Zemmour et al., 2010) (Figure 1). Co-immunoprecipitation assays identified a SRPX2-uPAR interaction, where SRPX2 interacted with the extracellular domains (DI-III) of uPAR *in vitro* (Royer-Zemmour et al., 2008a).

Like uPAR, SRPX2 has been linked with epileptogenic changes in both human and rodent brains (Roll et al., 2006; Sia et al., 2013). For instance, recent studies have associated two pathological mutations in the SRPX2 gene in humans with Rolandic epilepsy, oral and speech dyspraxia, mental retardation, and polymicrogyra (Roll et al., 2006, 2010). The SRPX2–uPAR interaction initiates neuronal migration and results in cortical excitability (Salmi et al., 2013). Both SRPX2 and uPAR are regulated by the binding of FOXP2 to their promoter region (MacDermot et al., 2005; Roll et al., 2010). The SRPX2-uPAR interaction activates P12k/Akt, Ras/MAPK, and P-FAK/Akt pathways leading to the activation of MMP2 and MMP9 metalloproteinases in cancer cells (Yamada et al., 2014; Tang et al., 2016; Lin et al., 2017; Liu et al., 2017). Therefore, the SRPX2-uPAR interaction and their converging functional roles make SRPX2 a favorable target for post-TBI tissue remodeling and repair. However, very little is known about the role of uPAR interactome or acquired factors in the regulation of SRPX2 expression.

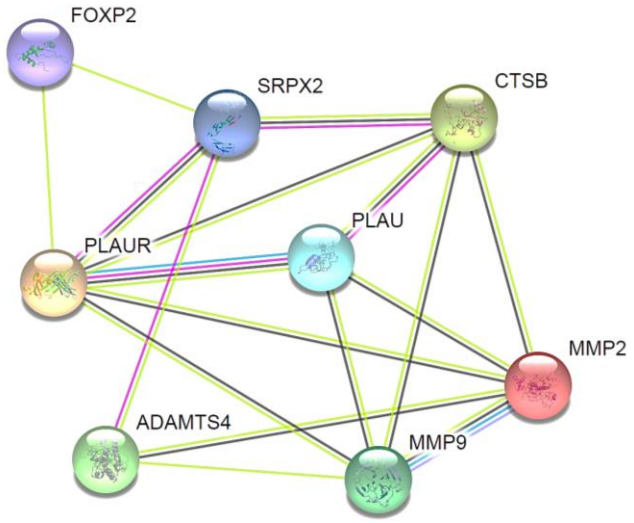

Figure 1. Evidence-based molecular interaction map of SRPX2 protein (generated using String version 11.0) summarizing the interplay of SRPX2 with key extracellular proteins.

Table 2. Studies describing the expression and role of SRPX2 in different human diseases

Disease	Sample type	Finding	Reference
Rolandic seizures, oral and speech dyspraxia, mental retardation	Blood	*SRPX2* gene mutations (N327S, Y72S)	(Roll et al., 2006)
Glioblastoma (GBM)	GBM brain tissue	Elevated SRPX2 mRNA and protein expression correlated with poor prognosis.	(Tang et al., 2016)
Language and motor delay, intellectual disability	Blood	*SRPX2* gene mutations (G751C, G762T)	(Schirwani et al., 2019)
Gastric cancer	Gastric mucosa	Elevated *SRPX2* expression correlated with tumor size.	(Tanaka et al., 2009, 2012; Yamada et al., 2014),
Colorectal cancer	Colon cancer tissue	Elevated SRPX2 expression correlated with clinical stage of disease.	(Liu et al., 2015)
Pancreatic cancer	Pancreatic ductal adenocarcinoma (PDAC) tissue	Elevated *SRPX2* expression in PDAC correlated with focal adhesion kinase (p-FAK) levels.	(Gao et al., 2015)
Hepatocellular carcinoma (HCC)	HCC tissue	Elevated SRPX2 mRNA and protein expression correlated with tumor stage.	(Lin et al., 2017)
Prostate cancer	Prostate cancer tissue biopsy	Elevated *SRPX2* expression	(Hong et al., 2018)
Esophageal squamous cell carcinoma (ESCC)	ESCC tissue	Elevated *SRPX2* expression	(He et al., 2019)

3 AIMS OF THE STUDY

The broad objective of this study is to understand the cellular and molecular reorganisation processes known to occur after a TBI. Furthermore, it aims to characterize the expression of a novel extracellular matrix protein, Sushi repeat-containing X-linked 2 (SRPX2) with and without TBI. Therefore, the specific aims of this work are to:

1. Study the spatial distribution of SRPX2 protein in normal rodent, non-human primate and human brain and its presence in plasma.

2. Determine whether uPAR or uPA deficiency affects SRPX2 expression in brain, and if this expression is differentially regulated after an experimental TBI.

3. Investigate the changes in SRPX2 expression in brain and plasma after an experimental TBI.

4. Examine the structural changes in hypophysis after an experimental TBI.

4 SUBJECTS AND METHODS

The aims and objectives of this thesis were achieved using four independent studies (I-IV) as shown in Figure 2.

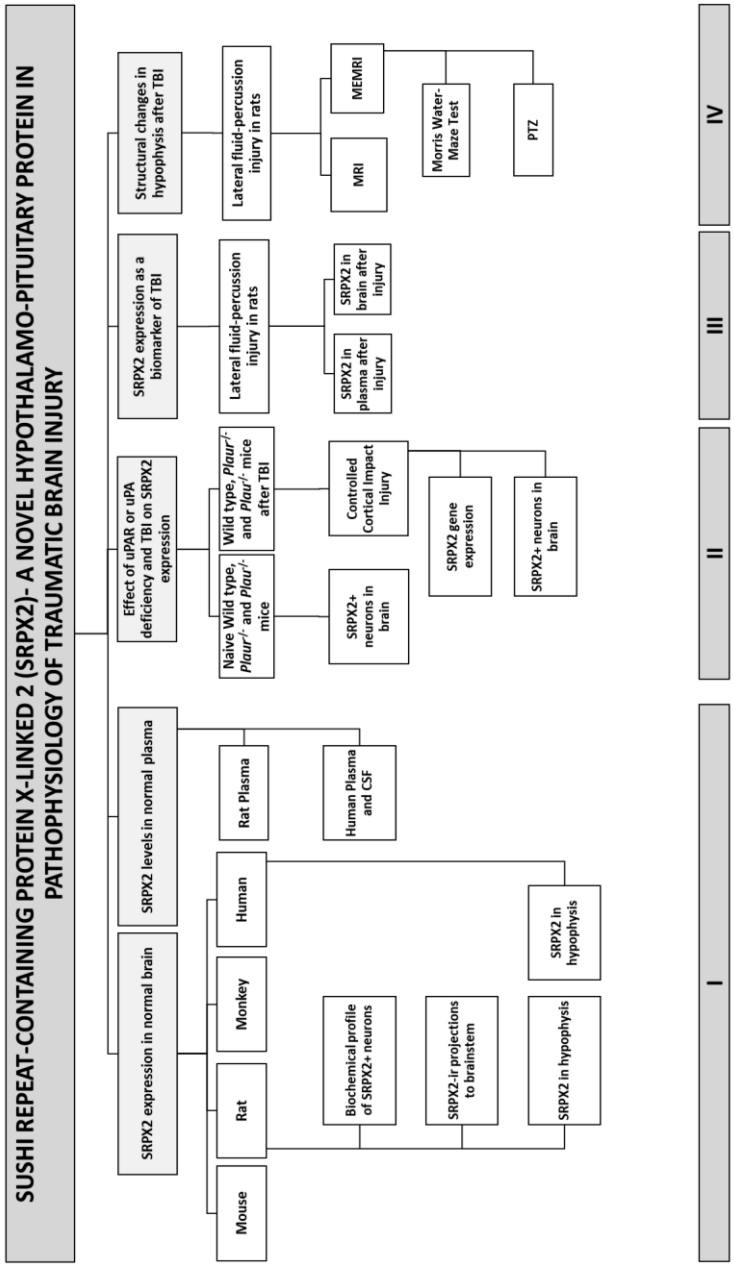

Figure 2. Schematic diagram showing an overview of all four studies included in the thesis.

4.1 OVERVIEW

An overview of the study subjects, experimental model, time points and methods employed in each study included in the thesis is provided in Table 3. The number of subjects used per experiment in each study can be found in Materials and Methods section of publications (I-IV) in Appendix 1.

Table 3. Overview of subjects, models of TBI and methods used in the thesis.

Study	Subjects	Animal models of TBI	Time-point	Sample used	Tissue Fixative	Methods employed
	Mice (C57BL/6J)		Naive	Brain	4% PFA	
	Rats (Sprague-Dawley)		Naïve	Brain Hypophysis Blood	4% PFA	
I	Monkey (*Macaca arctoides)*		Naïve	Brain	Ketalar and Nembutal cocktail	siRNA-based gene silencing RT-qPCR *In situ* hybridization Immunohistochemistry Immunofluorescence Western blot
	Human		Without a known neuro-pathology	Brain Hypophysis Blood CSF	10% formalin	
II	Mice (C57BL/6J, *Plaur*$^{-/-}$, *Plau*$^{-/-}$)	CCI	4 d and 14 d post-CCI	Brain	4% PFA	RT-qPCR Immunohistochemistry
III	Rats (Sprague-Dawley)	Lateral FPI	2 h, 6 h, 24 h, 48 h, 72 h, 5 d, 7 d, 14 d, 1 month, 3 months post-FPI	Brain Blood	4% PFA	Immunohistochemistry Western blot
IV	Rats (Sprague-Dawley)	Lateral FPI	2 d, 5 months, 8 months post-FPI		-	MRI MEMRI Morris water-maze PTZ

4.2 SUBJECTS AND ANIMALS

All animal procedures were approved by the Animal Ethics Committee of the Provincial Government of Southern Finland, and performed in accordance with the guidelines of the European Community Council Directives 2010/63/EU. The rodents

used in the study were not maintained under Specific-pathogen free (SPF) conditions. However, the animals were housed according to The Federation of European Laboratory Animal Science Associations (FELASA) recommendations for health monitoring of rodents and quarterly screened for harmful agents (Mähler et al., 2014).

The maintenance of the monkeys and all procedures conducted in the study were carried out according to the Finnish law and statutes governing animal experimentation. The Finnish Ministry of Agriculture approved the studies performed on monkeys.

Human brain, hypophysis, CSF and blood samples were obtained and used in accordance with the Declaration of Helsinki and Institutional Review Board approvals of Kuopio University Hospital, Academic Medical Center, University of Amsterdam and the Netherlands Brain Bank. Consent for autopsy was obtained in concordance with institutional regulations.

4.2.1 Humans (I)

Autopsy (24 hours post-mortem) human brain tissue (hypothalamus and hypophysis, n=5), from adult subjects without any diagnosed brain pathology (Male, 48-85 years old, cause of death: myocardial infarction) were obtained from Kuopio University Hospital, Kuopio, Finland, and Academic Medical Center, University of Amsterdam, The Netherlands and the Netherlands Brain Bank.

4.2.2 Monkeys (I)

Hypothalamic and brainstem sections from two female adult *Macaca arctoides* monkeys (age 5-6 years, weight 7-8 kg) were used for SRPX2 immunohistochemistry[1].

4.2.3 Rats (I, II, IV)

The animals were housed in a controlled environment (temperature 22 ± 1°C, humidity 50%–60%, light–dark cycle from 07.00 to 19.00 h) with free access to food and water. Adult (age 12-14 weeks, 290–450 g) male Sprague-Dawley rats (Envigo Laboratories S.r.l., Udine, Italy) were used to obtain brain tissue, plasma samples or MRI.

4.2.4 Mice (I-II)

The animals were housed in a controlled environment (temperature 22 ± 1°C, humidity 50%–60%, light–dark cycle from 07.00 to 19.00 h) with free access to food and water. Adult (12-14 weeks, 20–30 g) male C57BL/ 6J mice (The Jackson Laboratory, Bar

[1] The monkey brain sections were acquired from previously stored fixed frozen tissue stored at -80°C. The detailed procedures employed at the time of perfusion of monkeys are nonetheless presented in the following sections.

Harbor, ME, USA) were used to obtain brain tissue samples for SRPX2 immunohistochemical labelling **(I-II)**.

Male mice lacking the, uPAR encoding, *Plaur* gene in a C57BL/6J background (*Plaur* $^{-/-}$; originally from The Jackson Laboratories, B6.129P2-*Plaur*tm1Jld) and Wt mice were used. They were backcrossed to C57BL/6 genotype (Charles River, originally JAXC57BL/6J Stock 000664 from The Jackson Laboratory) for at least 8 generations. The genotypes of mice were determined by PCR. Breeding was continued as Wt or *Plaur*$^{-/-}$ homozygous lines (maximum of 10 generations before backcrossing) **(II)**.

Male mice lacking the, uPA encoding, *Plau* gene in a C57BL/6J background (*Plau*$^{-/-}$; B6.129S2-*Plau*tm1Mlg/J from The Jackson Laboratory, Bar Harbor, ME, USA) and Wt mice were used. Mice were backcrossed to the C57BL/6 genotype (The Jackson Laboratory) for at least eight generations. Mouse genotypes were determined by PCR. Breeding was continued as Wt or *Plau*$^{-/-}$ homozygous lines (maximum of 10 generations before backcrossing) **(II)**.

4.3 EXPERIMENTAL MODELS OF TBI

The effect of acquired brain injury on SRPX2 expression was investigated using two experimental models of TBI including CCI **(II)** and lateral FPI **(III-IV)**.

4.3.1 Induction of controlled cortical impact injury (II)

Mice (Wt, *Plaur*$^{-/-}$, *Plau*$^{-/-}$) were subjected to a unilateral cortical contusion as described earlier (Smith et al., 1995). Animals were anesthetized with sodium pentobarbital (60 mg/kg; single i.p. injection) and placed in a stereotaxic frame. The skull was exposed and a 5 mm craniotomy was performed over the left parieto-temporal cortex between lambda and bregma. The bone was carefully removed without disruption of the underlying dura. TBI was performed with a CCI device (eCCI-6.3; VCU Health System; Department of Radiology; Virginia Commonwealth University) equipped with an electrically driven metallic piston controlled by a linear velocity displacement transducer. CCI was delivered using the stroke (∅ 3 mm flat tip) parameters: depth 0.5 mm from dura, velocity 5 m/s, and dwell time 100 ms. Sham-injured animals received anesthesia and had craniotomy but were not exposed to CCI. After the injury, a piece of plastic was placed over the craniotomy and the incision was sutured.

4.3.2 Induction of lateral fluid-percussion injury (III-IV)

TBI was induced in rats using the lateral FPI (McIntosh et al., 1989a; Kharatishvili et al., 2006). Animals were anesthetized with with a cocktail (6 mL/kg, i.p.) of sodium pentobarbital (58 mg/kg), chloral hydrate (60 mg/kg;), magnesium sulfate (127.2 mg/kg), propylene glycol (42.8%), and absolute ethanol (11.6%). Chloral hydrate was no longer

allowed to be used as an anesthetic and was omitted from the anesthesia cocktail in some cohorts of study III and IV. Analysis showed no effect of anesthesia on the experimental outcome between cohorts (III-IV). Next, the animals were placed in a stereotaxic frame (David Kopf Instruments, Tujunga, CA, USA) and the skull was exposed. A circular craniectomy (⌀ 5 mm) over the left parietal lobe midway between lambda and bregma was performed leaving the dura intact. Lateral FPI (impact severity, 2.8-3.8 atm) was induced by connecting the rat to the fluid-percussion device (AmScien Instruments, Richmond, VA, USA). Sham operated animals went through the same procedure except the lateral FPI.

4.4 PROCESSING OF TISSUE FOR HISTOLOGY

4.4.1 Humans (I)

For immunohistochemistry, the hypothalamus and hypophysis were fixed in 10% formalin solution for 48 h, followed by cryoprotection for 48 h in a solution containing 20% glycerol and 2% DMSO in 0.1 M sodium phosphate buffer. The tissue was then immersed in ice-cold isopentane, and frozen blocks were stored at -70°C until cut (Blümcke et al., 2016). The blocks containing hypothalamus and hypophysis were cut into 30-μm-thick coronal sections (1-in-8 series) using a sliding microtome. Free-floating sections were stored at -70°C in tissue collecting solution (TCS: 30% ethylene glycol, 25% glycerol in 0.05 M sodium phosphate buffer) until used for immunohistochemistry.

For *in situ* hybridization, 6-μm-thick coronal sections were cut from paraffin embedded human hypothalamic tissue and collected on glass slides. The slides were dried and stored at RT until use.

4.4.2 Monkeys (I)

The monkeys were deeply anesthetized with a cocktail of Ketalar (1ml) and Nembutal (4.5ml). The animals were perfused intracardially with 0.9% saline (250ml/min) for 2 min at RT followed by a solution of 4% PFA and 0.1% glutaraldehyde in 0.1 M sodium phosphate buffer for 10 min at the rate of 250ml/min and then 50 min at the rate of 100ml/min. The brain was removed from the skull and post-fixed for 2 h at 4°C in the above fixative. The brain tissue was then cryoprotected in 10% glycerol and 2% dimethylsulfoxide (DMSO) solution for 24 h, in 20% glycerol and 2% DMSO solution for 3 days at 4°C, and then frozen by immersion in ice cold isopentane (2-methyl butane)(Caston-Balderrama et al., 1998). Coronal sections of the brain (30 μm) were cut in a 1-in-8 series and stored in TCS at -70°C until stained.

4.4.3 Rats and mice (I-III)

For immunohistochemistry, the tissue was processed as previously described (Ndode-Ekane et al., 2010). Briefly, the mice were deeply anesthetized with a mixture of

18.75 mg/mL ketamine and 0.25 mg/mL medetomidine (4 mL/kg, i.p.) and rats with a cocktail of sodium pentobarbital (58 mg/kg), magnesium sulfate (127.2 mg/kg), propylene glycol (42.8%), and absolute ethanol (11.6%) (6 mL/kg, i.p.). The animals were transcardially perfused with 0.9% saline (mice: 5 ml/min, rats: 30 ml/min at 4°C) for 3 min followed by 4% PFA in 0.1 M sodium phosphate buffer, pH 7.4 (mice: 5 ml/min, rats: 30 ml/min at 4°C), for 15 min. The brain (and hypophysis where possible) was removed from the skull and post-fixed in 4% PFA for 4 h (at 4°C), and then cryoprotected in a solution containing 20% glycerol in 0.02 M potassium phosphate buffered saline (KPBS) for 24 h. The brains were then frozen on dry ice and stored at -70°C until cut. The mouse and rat brains were sectioned in a coronal plane (25-30 μm) with a sliding microtome (Leica SM 2000, Leica Microsystems Nussloch GmbH, Nussloch, Germany). The first series of sections was collected in 10% formalin at room temperature (RT) for thionin staining. The remaining series of sections were stored in tissue collecting solution (TCS: 30% ethylene glycol, 25% glycerol in 0.05 M sodium phosphate buffer) at -20°C until staining.

For *in situ* hybridization, rat brains were fixed in 10% buffered formalin and embedded in paraffin. Sagittal sections (6 μm) were cut using a microtome, collected on glass slides, and stored at room temperature (RT) until use.

4.5 ANTIBODY SPECIFICITY (I)

As there were no prior reports on validation of antibody against SRPX2, the specificity of rabbit anti-SRPX2 antibody (ab91584, Abcam) used for the immunostaining, was confirmed by *in vitro* siRNA based silencing of SRPX2 in cell cultures. The antibody specificity strategy was determined using the guidlines of according to the recommendations of International Working Group for Antibody Validation(Uhlen et al., 2016). SRPX2 immunostainings were compared between untransfected, mock transfected and SRPX2 siRNA transfected cells using immunofluorescence and western blotting.

Firstly, endogenous SRPX2 expression was determined in mouse N2a neuroblastoma cell line, human n2012 teratocarcinomas cells, and human SH-SY5Y neuroblastoma cells. Since SH-SY5Y cells expressed *SRPX2* mRNA abundantly, these cells were selected for transfection with *SRPX2* siRNA for antibody validation. SH-SY5Y cells were cultured as previously described (Kovalevich and Langford, 2013).

For siRNA transfection, cells were plated into 12-well plates (150,000 cells/well) and allowed to adhere overnight. Colorimetric 3-(4,5-dimethylthiazol-2)-2,5-diphenyltetrazolium bromide (MTT, M2128, MilliporeSigma) cell viability assay was used to determine transfection-induced cytotoxicity as described previously (Deng et al., 2005). Pre-designed *Silencer*® siRNA against human *SRPX2* mRNA (AM16708, Ambion) was transfected into SH-SY5Y cells using Lipofectamine® 2000 (Thermo Fisher Scientific). In order to ensure transfection efficiency and specificity, *Silencer*® FAM-labeled negative control siRNA (AM4620, Ambion) was transfected in parallel to *SRPX2*

siRNA. Transfection was carried out using the manufacturer's protocol. Transfection outcome was evaluated using RT-qPCR followed by western blot and immunofluorescence staining.

For RT-qPCR, total RNA was extracted using AllPrep DNA/RNA Mini Kit (QIAGEN®, Hilden, Germany), followed by quantification by NanoDrop™ (ND-1000). cDNA was synthesized using high-capacity RNA-to-cDNA Kit (Applied Biosystems, Foster City, CA, USA) and amplified using TaqMan® Gene Expression Master mix (Applied Biosystems). The human SRPX2 TaqMan® gene expression assay (Hs00997580, Thermo Fisher Scientific) was used for *SRPX2* mRNA amplification. β-actin was measured simultaneously (Armstrong et al., 2007) as a stable endogenous control using the human ACTB TaqMan® assay (Hs03023943-g1, Thermo Fisher Scientific). All assays were performed according to the manufacturer's protocol. *SRPX2* mRNA level values were normalized to *ACTB* mRNA levels and expressed as fold-increases relative to gene expression in untreated control cells.

After confirming transfection with RT-qPCR, the transfection was repeated and cells were used to evaluate the specificity of rabbit polyclonal antibody raised against human SRPX2 (ab91584, Abcam) by ***Western blotting*** (Sutiwisesak et al., 2014). 1x RIPA lysis buffer containing a protease inhibitor cocktail was added to the wells containing transfected frozen SH-SY5Y cells for 30 min. The cell debris was palleted by centrifuging the lysate at 2,800g for 15 min at 4°C and the supernatant was stored at -70°C until use. A mixture of lysate (20 μg of protein), 1X Laemmli buffer, and β-mercaptoethanol was heated at 90°C, separated by SDS-polyacrylamide gel electrophoresis (SDS-PAGE) and transferred to PVDF membranes. The membranes were blocked for 2 h in 1X TEN-1% Tween20 solution and incubated overnight at 4°C with rabbit polyclonal anti-SRPX2 (1:1000, ab91584, Abcam) or mouse monoclonal anti-β-actin (1:1000, sc-47778, Santa Cruz Biotechnology, Dallas, TX, USA) antibody. The blots were then incubated with HRP goat anti-rabbit (1:2000, 65-6120, Invitrogen) and goat anti-mouse (1:2000, 62-6520, Invitrogen) secondary antibodies for 1h at RT. Immunoreactive bands were visualized using enhanced chemiluminescence substrate (ECL, SuperSignal™ West Pico Chemiluminescent Substrate, Thermo Fisher Scientific) on a gel documentation system (GelDoc Bio-Rad).

For immunofluorescence staining, SH-SY5Y cells were grown on coverslips in 12 well plates. The cells were rinsed with PBS, fixed in 4% PFA solution for 15 min (at RT), rinsed with 1x PBS, permeabilized with 0.1% Triton-X100 for 2 min, and then incubated with the rabbit anti-SRPX2 antibody (1:1000, ab91584, Abcam) for 1 h. The cells were then incubated with anti-rabbit Alexa488 (1:200, ab150117, Abcam) or anti-rabbit Alexa568 secondary antibody (1:200, ab175695, Abcam) for 1 h at RT (Acosta et al., 2009). The coverslips were mounted on glass slides and sealed with VectaShield containing DAPI (H-1200, Vector).

4.6 *IN SITU* HYBRIDIZATION (I)

SRPX2 mRNA *in situ* hybridization was performed on rat and human hypothalamic sections using 5′–3′ double digoxygenin (DIG)-labeled probe, containing locked nucleic acid [LNA] and 2′O-methyl [2′Ome] RNA moieties (Exiqon, Vedbaek, Denmark) as described before (Prabowo et al., 2015). In order to detect both rat (NM_001108243.2) and human (NM_014467.2) *SRPX2* mRNA using the same probe, a conserved sequence) was used in designing the probe. Hybridization was carried out by incubating the sections with the *SRPX2* mRNA probe (250 nM) at 56°C for 1 h. To detect the SRPX2 mRNA hybridization, NBT (nitro-blue tetrazolium chloride)/BCIP (5-bromo-4-chloro-30-indolyphosphate p-toluidine salt) was used as chromogenic substrate for anti-DIG alkaline phosphatase (AP). The slides were mounted with VectaMount at RT.

To visualize both *SRPX2* mRNA and protein simultaneously, *in situ* hybridization was followed by immunohistochemistry. After developing the chromogenic reaction for *SRPX2* mRNA, the sections were incubated with horseradish peroxidase (HRP)-labeled anti-rabbit secondary antibody (BrightVision+ kit, DPVB110HRP, Immunologic, Duiven, the Netherlands) and antigen was visualized by chromogen 3-amino-9-ethylcarbazole (AEC, A-5754, MilliporeSigma) Negative control assays were performed without probes and the primary antibody. These sections were blank and showed no immunoreactivity.

4.7 IMMUNOHISTOCHEMISTRY (I-III)

4.7.1 SRPX2 and oxytocin immunohistochemistry (I-III)

SRPX2 and oxytocin protein were detected using immunohistochemistry in a 1-in-5 series of coronal sections as previously described (Ndode-Ekane et al., 2010). The sections were first washed in 0.02 M KPBS (pH 7.4) and incubated with 1% H_2O_2 to reduce the endogenous peroxidase activity followed by blocking in 10% NGS and 0.5% Triton X-100. The sections were then incubated in a mixture of primary antibody (rabbit polyclonal antibody raised against SRPX2 (1:10,000, ab91584, Abcam, Cambridge, UK, RRID: AB_2050340 or rabbit anti-oxytocin antibody (1:16,000, AB911, MilliporeSigma), 1% NGS, and 0.5% Triton X-100 in KPBS for 2 nights at 4°C. After washing with KPBS, the sections were then incubated for 1 h in biotinylated goat anti-rabbit IgG antibody (1:200, BA-1000, Vector Laboratories, Burlingame, CA, USA). The sections were subsequently incubated in 1% avidin-biotin enzyme complex ABC (Vectastatin® ABC kit, PK4000, Vector Laboratories) solution for 45 min. To visualize the antigen, 0.1 % 3,3′-diaminobenzidine (Pierce Chemical, Rockford, IL, USA) solution containing 0.4% H_2O_2 in KPBS was added to the sections for 1 min. The sections were transferred to glass slides and dried overnight at 37°C. The staining reaction was intensified using 0.005% osmium tetroxide (OsO4, #19170, Electron Microscopy Sciences, Hatfield, PA, USA) as

previously described (Lewis et al., 1986). The slides were covered with Depex® and dried overnight in the hood.

For SRPX2 immunohistochemistry in monkey and human brain tissue, the same protocol was used, except that the sections were pre-treated with 1% sodiumborohydride for 15 min before blocking. In human, sections containing hypothalamus were stained. In monkeys, sections including the brainstem were also stained.

4.7.2 Quantitative analysis (I-III)

SRPX2 immunopositive cells throughout the rostrocaudal axis of hypothalamus were plotted using the AccuStage MDPlot 5.3 software and MD3 Microscope Digitizer (AccuStage, Shoreview, MN, USA) connected to a Leica DMRB microscope. The cytoarchitectonic boundaries of paraventricular (Pa), periventricular (Pe), and supraoptic (SO) nuclei were then drawn on computer-generated plots from the adjacent thionin-stained sections with the aid of a *camera lucida* stereomicroscope equipped with a drawing tube. The total number of cells (N_{tot}) was calculated per region (Pa, Pe, and SO) according to the following formula: $N_{tot} = \sum Q \times 1/ssf$, where $\sum Q$ is the sum of cells counted from all sections and ssf is the section sampling fraction (1/5) (West et al., 1991). Data is expressed as mean ± SEM.

To estimate the number of SRPX2-ir granules per SRPX2-ir neuron, 8-10 bright-field photomicrographs were captured from hypothalamic Pa and So nuclei from two naïve and three 2 h post-TBI rat brains using 100x magnification, resulting in 2-3 cells per photomicrograph for the estimation. The images were converted to gray scale and the number of immunolabeled granules per SRPX2-ir neuron was counted in the Pa and SO nuclei on the ipsilateral and contralateral side of the hypothalamus.

To estimate the density of SRPX2-ir fibers in the hypothalamus, two dark-field successive photomicrographs showing SRPX2-ir projections were captured from three naïve and three 2 h post-TBI rat brains using 10x magnification. The images were acquired with the same light settings and converted to 8-bit gray scale and threshold. A region of interest (ROI) covering the SRPX2-ir projections was drawn on the ipsilateral and contralateral side of each section. Background was subtracted from each photomicrograph and mean gray values were acquired.

4.8 IMMUNOFLUORESCENCE (I)

To identify the cell types expressing SRPX2, rat hypothalamic sections were double-labeled with either oxytocin, vasopressin, GFAP or OX-42 antibodies (Table 4). Sections were washed with KPBS and incubated with 1% NGS in KPBS containing 0.5% Triton X-100, and then, incubated overnight with 1st primary antibody. After washing with PBS, the sections were incubated with fluorescent secondary antibody against 1st primary antibody for 2 h, washed again with PBS and incubated overnight with 2nd

primary antibody. The sections were washed in PBS and then incubated with fluorescent secondary antibody against 2nd primary antibody. Sections were washed, mounted and cover-slipped with VectaMount and sealed with nail enamel.

Table 4. Summary of antibodies used for immunofluorescent double labelling of rat brain tissue.

Double labelling	Primary Antibody	Dilution	Secondary Antibody	Dilution
SRPX2 and Oxytocin	Rabbit anti-SRPX2 (ab91584, Abcam)	1:1000	anti-rabbit Alexa488 (ab150077, Abcam)	1:200
	Mouse anti-Oxytocin (MAB5296, MilliporeSigma)	1:5000	anti-mouse Alexa 647 (ab150115, Abcam)	1:200
SRPX2 and Vasopressin	Mouse anti-SRPX2 (66266-1, Proteintech)	1:1000	anti-mouse Alexa 488 (ab150117, Abcam)	1:200
	Rabbit anti-Vasopressin (AB1565, Chemicon)	1:5000	anti-rabbit Alexa 568 (ab175695, Abcam)	1:200
SRPX2 and GFAP	Mouse anti-GFAP (814369, Boehinger Mannheim)	1:2000	anti-mouse Alexa 488 (ab150117, Abcam)	1:200
	Rabbit anti-SRPX2 (ab91584, Abcam)	1:5000	anti-rabbit Alexa 568 (ab175695, Abcam)	1:200
SRPX2 and OX-42	Mouse anti-OX-42 (MCA275G, Bio-Rad)	1:2000	anti-mouse Alexa 488 (ab150117, Abcam)	1:200
	Rabbit anti-SRPX2 (ab91584, Abcam)	1:5000	anti-rabbit Alexa 568 (ab175695, Abcam)	1:200

To estimate the percentage of SRPX2 positive cells that also express oxytocin, 10 photomicrographs were captured from 3 rat brains (2 sections from each animal) using 40x magnification, resulting in 5-10 cells per photomicrograph for colocalization estimation. The number of immunolabeled cells for each antibody was counted in the Pa and SO nuclei of the hypothalamus.

4.9 NISSL STAINING (I-III)

To identify the cytoarchitectonic boundaries of different brain areas, the sections was used for Nissl staining (Huusko et al., 2015). The sections were mounted on gelatin (0.5%, G-2500, MilliporeSigma, Burlington, MA, USA) coated glass slides, rehydrated in decreasing grades of alcohol, stained for thionin, dehydrated in increasing grades of alcohol and cover-slipped with mounting medium (Depex® BDH Chemical, Poole, UK).

4.10 PLASMA AND CEREBROSPINAL FLUID SAMPLES (I, III)

Plasma and CSF samples were obtained for western blot analysis. For rat plasma, blood samples were obtained from the lateral tail vein of adult male rats under isoflurane anesthesia. The samples were centrifuged (1,300g for 10 min at 4°C), plasma was aliquoted and stored at -70°C until used. For human plasma samples, blood samples were obtained from the cubital vein of healthy adult male and female subjects (n=3) at Kuopio University Hospital between 7 am – 8 am. The samples were centrifuged (2,200g for 10 min at RT), plasma was collected and stored at -70°C. CSF samples were obtained from adult human cases without any diagnosed neuropathology [2] (n=3) through lumbar puncture performed at Kuopio University Hospital between 9 am – 11 am. After brief mixing, the samples were centrifuged (2,000g for 10 min at RT), supernatant was collected and stored at -70°C.

4.11 WESTERN BLOT (I, III)

Pierce BCA Protein Assay Kit (23225, Thermo Fisher Scientific) was used to measure the total protein concentration in plasma and CSF. Plasma samples were diluted with PBS and the diluted plasma (20 μg protein, final volume 25 μl) or 60 μl undiluted CSF, 1X Laemmli buffer, and β-mercaptoethanol were heated at 90°C, separated on 12% TGX Stain-Free™ gels (Bio-Rad, Hercules, CA, USA) by SDS-polyacrylamide gel electrophoresis (SDS-PAGE) and transferred to PVDF membranes. Membranes were blocked 1X TEN-1% Tween20 solution and incubated with rabbit polyclonal anti-SRPX2 (1:1000, ab91584, Abcam) overnight at 4°C. The blots were then incubated with HRP goat anti-rabbit (1:10000, 65-6120, Invitrogen, Carlsbad, CA, USA) antibody for 1 h at RT. ECL substrate was used to visualize SRPX2 immunoreactive bands on a gel documentation system.

Western blot data from the rat plasma samples after FPI-induced injury were analyzed following the guidelines provided by Taylor and co-workers (Taylor et al., 2013) **(III)**. The linearity and limit of detection of anti-SRPX2 antibody was determined and a reliable immunoreactive signal up to 5 ug of total protein was observed. Negative control assay showed no immunoreactivity. To minimize the inter-membrane effect, a naïve plasma sample was run as a positive control in all gels. Images were captured from (i) the stain free gels after SDS-PAGE, (ii) the membranes after protein transfer, and (iii) the immunostained blot at same exposure time and resolution. The images were analyzed using ImageJ software. For the quantitative estimation of SRPX2 levels in plasma, the acquired images were converted to 8-bit gray scale. A region of interest (ROI) containing the SRPX2 band at 53 KDa was drawn and was used on all blot images. Mean gray values of the ROI were acquired and background was subtracted. The values

[2] Tap-test (CSF removal) was requested by the clinician due to suspected idiopathic normal pressure hydrocephalus (iNPH).

were then normalized for total protein as loading control and the positive control to minimize inter-membrane variability.

4.12 MAGNETIC RESONANCE IMAGING (IV)

MRI scans were acquired as reported previously (Ndode-Ekane et al., 2010). Rats were anesthetized using 1.5-2% isoflurane (carrier gas mixture of 70% N_2 and 30%O_2) and were secured in a holder using ear bars and a bite bar while anesthesia was delivered through a nose cone. Breath rate and body temperature were monitored. Animals were first scanned at 2 days (d) post-TBI and then a follow-up MRI scan was done at 5 months post-TBI. MRI was performed with a 7 T scanner (Bruker Pharmascan, Billerica, MA) operated with ParaVision 5.1 software. An actively decoupled quadrature resonator volume transmitter coil and a rat brain quadrature surface receiver coil (Rapid Biomedical, Germany) were used to acquire high resolution structural 3D MRI. A multi echo gradient echo (MGE) sequence with 66 ms repetition time, flip angle of 16 degrees, field of view 25.6 x 19.5 x 12.8 mm, matrix 160 x 122 x 80, 1 average, 120 dummy scans to obtain steady state, outer volume suppression and fat suppression was used. Thirteen echoes with echo time ranging from 2.7 ms to 43 ms with a 3.1 ms interval were collected, and all 13 echo images were summed together. This resulted in T1/T2* mixed contrast and 160 x 160 x 160 μm^3 spatial resolution.

The region of interest (ROI) outlining the hypophysis was manually drawn in the sagittal plane using ImageJ software (National Institute of Health, USA, version 1.51j8) and the total hypophyseal volume was assessed. Total volume was calculated by multiplying the total number of pixels with the size of each pixel. The data are expressed as mm^3.

4.13 $MnCl_2$-ENHANCED MRI (MEMRI) (IV)

The volumes of individual hypophyseal lobes were estimated from MEMRI scans. Rats were anesthetized and prepared as stated in section 4.12. At 8 months post-TBI, MRI was performed with a 4.7 T scanner (Magnex Scientific Ltd, Abington, UK) interfaced to a Varian console (Varian Inc., Palo Alto, CA). An actively decoupled volume transmitter coil and a quadrature surface receiver coil were utilized (Hayward et al., 2010). Manganese enhanced images were acquired 24 hours after systemic $MnCl_2$ injection (intraperitoneal injection, 54 mg/$MnCl_2.4H_2O$/kg in 0.1 M bicine buffer, pH 7.4) (Jackson et al., 2011). T1 weighted 3D MEMRI images were obtained with a gradient echo sequence of repetition time 1200 ms, echo time 4 ms, 70 degrees flip angle, field of view 35 x 35 x 25 mm, matrix 256 x 270 x 64 zerofilled to 256 x 270 x 256 resulting in 137 x 130 x 98 μm resolution.

ROIs were drawn in the coronal plane to estimate the volume of the adenohypophysis (intermediate lobe included) and neurohypophysis separately. Total

volume was calculated by multiplying the total number of pixels with the size of each pixel. The data are expressed as mm^3.

4.14 PENTYLENETETRAZOL TEST (IV)

In order to assess susceptibility to induced seizures, PTZ test was performed (Hayward et al., 2010). Rats were injected with a single dose (25 mg/kg) of PTZ (1,5-pentamethylenetetrazole, 98%, Sigma-Aldrich YA-Kemia Oy, Finland). Rats were placed in individual transparent plexiglass cages and video-EEG was recorded for 60 min after PTZ administration. An electrographic seizure was defined as a >5 sec duration high-amplitude rhythmic discharge with a clear onset, temporal evolution in wave morphology and amplitude, and offset. PTZ-induced epileptiform discharges were defined as a high amplitude rhythmic discharge containing a burst of slow waves, spike-wave and/or polyspike-wave components and lasting <5 sec. A spike was defined as a high-amplitude (twice baseline) sharply contoured waveform with a duration of 20-70 msec. Latency to the first spike, total number of spikes, total number of epileptiform discharges and the total number of electrographic seizures were calculated.

4.15 MORRIS WATER-MAZE TEST (IV)

Hippocampus-dependent learning and memory were assessed as previously described using the Morris water-maze (Karhunen et al., 2003; Hayward et al., 2010, 2011). Briefly, the test was conducted in a black pool of water (150 cm, 20 ± 2°C) surrounded by visual clues for animals to orient themselves. The pool was divided into four quadrants, and a platform was placed 1.5 cm below the water in the middle of the northeast quadrant. A video camera connected to a computerized image analysis system (HVS image, Imaging Research Inc., UK) was positioned above the pool. The rats were tested on three consecutive days, with five trials per day on days 1 and 2. The swimming start position was altered in every trial and if a rat failed to find the platform within 60 sec, it was guided to the target manually. Rats were allowed to remain on the platform for 10 sec after each trial. Thereafter, it rested in its cage for 30 sec (after trials 1, 2, and 4) or 1 min (after trials 3 and 5). On day 3, the platform was removed to assess the ability of rats to remember the location of the platform. The latency to the platform (maximum 60 sec), length of the swimming path during the trial (cm), mean swimming speed (cm/sec) and percentage total time spent in each of the four quadrants were measured.

4.16 STATISTICAL ANALYSIS (I-IV)

Data was analyzed using IBM SPSS 25.0 for Windows (SPSS Inc., IL, USA). Differences between the groups were analyzed using the Mann-Whitney U-test. Interhemispheric differences were analyzed using Wilcoxon's test. Correlations were

assessed using Spearman's rho correlation coefficient. Receiver operating characteristics (ROC) analysis was performed to assess the sensitivity and specificity of plasma SRPX2 levels and number of SRPX2-ir in the hypothalamus to discriminate the rats with injury from controls. Data are expressed as mean ± standard error of the mean (SEM). A p-value of less than 0.05 was considered statistically significant.

4.16.1 Unsupervised hierarchial clustering analysis (II-III)

To investiage the possibility of identifying the different sub-groups of animals clustered together based on SRPX2 expression, unsupervised hierarchical clustering was performed in R environment (version 3.0.1) (http//www.R-project.org/) using the Gplots package. Animals were ordered in a clustering heat map with the single-linkage method together with the Manhattan distance measurement as previously described (Bolkvadze et al., 2016). Clusters were identified from the dendrograms.

5 RESULTS

5.1 SPECIFICITY OF SRPX2 ANTIBODY (I)

First, the specificity of the antibody (polyclonal rabbit anti-SRPX2, ab91584, Abcam) used for SRPX2 immunolabeling was confirmed using small interfering RNA (siRNA) in the human SH-SY5Y neuroblastoma cell line to silence the *SRPX2* mRNA **(I, Fig. 1)**. The transfection efficiency was evaluated using a FAM-labeled negative control siRNA, which was detected, in the cells 24 h after transfection. A post-transfection cell viability assay showed a 17% decrease in cell numbers in transfected group when compared to untreated cells. This change was comparable in all transfections and not due to anti-SRPX2 siRNA transfection**.**

RT-qPCR analysis showed a dose-dependent reduction in the *SRPX2* mRNA following transfection. The knockdown percentage (%KD) of *SRPX2* mRNA was 54% using 30 nM and 87% using 50 nM *SRPX2* siRNA as compared with untreated cells after normalization with the internal control *ACTB*. The mock transfection at the same concentrations did not result in *SRPX2* mRNA reduction **(I, Fig. 1)**.

Like RT-qPCR, western blot showed a reduction in the intensity of 53 Kda immunolabeled band indicating dose dependent reduction in SRPX2 protein levels post-transfection. Immunofluorescence staining using the same anti-SRPX2 antibody showed a marked reduction in SRPX2 immunolabeling in SH-SY5Y cells transfected with 50 nM siRNA as compared with untreated and mock-transfected cells **(I, Fig. 1)**. The reduction in SRPX2 protein detection by anti-SRPX2 antibody after siRNA based *SRPX2* gene silencing confirmed the specificity of the antibody.

5.2 SRPX2 IS EXPRESSED IN NORMAL BRAIN (I)

In order to identify the precise location of SRPX2 mRNA in a normal brain, sections from rat and human brains were labeled using *in situ* hybridization. SRPX2 expression were detected in the hypothalamic paraventricular (Pa), periventricular (Pe) and supraoptic (SO) nuclei. Next, the brain sections were immunolabeled for SRPX2 protein, which showed a prominent immunoreactivity in the same regions of the rat and human hypothalamus. SRPX2 expression was cytoplasmic and only detected in neurons. Double labelling with *in situ* hybridization and immunohistochemistry confirmed the colocalization of SRPX2 mRNA and SRPX2 protein in the same cells. SRPX2 immunolabeling in the hypothalamic sections was reproduced with another antibody against SRPX2 protein (mouse monoclonal anti-SRPX2 antibody, 66266-1, Proteintech). Contrary to previous reports, no SRPX2 immunoreactivity was detected in the rat and human cortex. However, RT-qPCR revealed a relatively weak *SRPX2* mRNA expression in human cortex as compared with the hypothalamus **(I, Fig. 2).**

5.3 HYPOTHALAMIC SRPX2 EXPRESSION IS HIGHLY CONSERVED AND CAN BE DETECTED IN PLASMA (I)

In rat brain, all SRPX2-ir neurons were located in the hypothalamus particularly in the Pa, Pe and SO nuclei. SRPX2-ir neurons were distributed bilaterally in all functional compartments of Pa nucleus including the neurosecretory magnocellular neurons, endocrine and pre-autonomic parvocellular neurons. In the Pe, SRPX2-ir cells were scattered along its complete rostro-caudal axis. The SO nucleus exhibited strong SRPX2 immunoreactivity and a few scattered SRPX2-ir neurons were observed in the supraoptic decussation part and the nucleus circularis. The cytoplasmic SRPX2 protein had a granular appearance when observed at a higher magnification. Stereological cell counting revealed 2495 ± 215 SRPX2-ir neurons in the Pa (32% of all SRPX2-ir neurons in the hypothalamus), 835 ± 94 in the Pe (11% of all ir neurons), and 4520 ± 292 in the SO nucleus (58% of all ir neurons) **(I, Fig. 3)**.

Dense SRPX2-ir projections from the hypothalamic SRPX2-ir neurons traveled ventrally and caudally towards the hypophysis and SRPX2-ir passing fibers were exclusively localized in the internal layer of the median eminence. Light projections to the dorsal and ventral raphe, locus coeruleus, and nucleus of the solitary tract were also observed. Few immunolabeled fibers traveled through the pontine reticular nucleus and the intermediate reticular nucleus. Very few SRPX2-ir fibers were observed in the lateral septal nucleus and the anteroventral periventricular nucleus. A very light short varicose SRPX2 projection was found in the dorsal part of the central division of the medial nucleus and in the anterior cortical nucleus of the amygdaloid complex. No axonal staining was found in the cerebral cortex **(I, Fig. 4)**.

Like in rat, also in the mouse brain SRPX2-positive neurons were exclusively located in the hypothalamus. The estimated total number of SRPX2-ir neurons in the mouse hypothalamus was 1843 ± 303 in the Pa, 503 ± 85 in the Pe, and 837 ± 108 in the SO nuclei. Also like in rat, no immunoreactivity was detected in the cortex. The analysis of monkey and human hypothalamic sections indicated that the spatial distribution of hypothalamic SRPX2-ir neurons was consistent among rodents and primates **(I, Fig. 3)**.

Oxytocin and vasopressin are synthesized in the Pa and SO nuclei, transported to the hypophysis and secreted into the blood stream (Swanson and Sawchenko, 1983). In view of location of SRPX2-ir neurons in Pa and SO, a double-labeling of SRPX2 with oxytocin or vasopressin was performed in the rat hypothalamus. About 88% of SRPX2-ir neurons in the Pa and 61% in the SO were also immunoreactive for oxytocin. Double immunofluorescence also indicated colocalization of SRPX2 with vasopressin **(I, Fig. 5)**.

In rat neurohypophysis, dense SRPX2-ir terminal arborizations were observed. In the human neurohypophysis, SRPX2 immunoreactivity was observed in the terminals and axonal Herring bodies. The cells in the rat and human adenohypophysis exhibited cytoplasmic vesicle-like SRPX2 immunoreactivity **(I, Fig. 5)**.

After determining the distribution of SRPX2 in the brain, it was investigated whether SRPX2 protein is present in rat and human blood, and CSF. A 53 kDa SRPX2 immunoreactive band was detected in rat and human plasma with two different SRPX2 antibodies using western blot. SRPX2 protein was also detected in human CSF from the same cases. SRPX2 protein was detected in both male and female human plasma and CSF samples **(I, Fig. 5)**.

5.4 SRPX2 EXPRESSION IS REGULATED INDEPENDENT OF UPAR (II)

In order to understand the role of the uPAR interactome in the regulation of SRPX2 expression in brain, SRPX2 expression was assessed in wildtype mice and mice with uPAR (*Plaur*$^{-/-}$) or uPA (*Plau*$^{-/-}$) deficiency.

Srpx2 mRNA was detected in both Wt and knockout mice. However, the *Srpx2* gene expression in hypothalamus, cortex, hippocampus and thalamus did not differ between Wt, *Plaur*$^{-/-}$ and *Plau*$^{-/-}$ mice ($p>0.05$) **(II, Table 1 and Fig. 4)**. To further investigate the effect of uPAR or uPA deficiency on SRPX2 expression, SRPX2 immunoreactvity in brain was investigated. Similar to normal mouse brain, SRPX2-ir neurons were distributed bilaterally in hypothalamic Pa, Pe and SO nuclei of *Plaur*$^{-/-}$ and *Plau*$^{-/-}$ mice **(II, Fig. 2)**. No immunoreactivity was detected in cortex, hippocampus or thalamus.

The total number of SRPX2-ir neurons in the hypothalamus of *Plaur*$^{-/-}$ mice (2985 ± 138 vs 2890 ± 92) was comparable to that of the Wt mice ($p>0.05$). Nucleus-specific analysis indicated that the number of SRPX2-ir neurons in the hypothalamic Pa (1820 ± 270 vs 1906 ± 24), Pe (405 ± 60 vs 260 ± 53) and SO (760 ± 113 vs 723 ± 125) nuclei of *Plaur*$^{-/-}$ mice did not differ from that in Wt littermates ($p>0.05$) **(II, Fig. 2)**.

The total number of SRPX2-ir neurons in hypothalamus of *Plau*$^{-/-}$ mice (2026 ± 77 vs 2180 ± 232) was comparable with the Wt mice ($p>0.05$). The number of SRPX2-ir neurons in the hypothalamic Pa (1200 ± 81 vs 1750.3 ± 210), Pe (206 ± 21 vs 180 ± 16) and SO (620 ± 128 vs 250 ± 48) nuclei of *Plau*$^{-/-}$ mice was comparable to that in their Wt littermates ($p>0.05$) **(II, Fig. 2)**.

Taken together, the *Srpx2* mRNA and SRPX2 protein expression in Wt, Plaur$^{-/-}$ and Plau$^{-/-}$ mice was comparable and no genotype effect was found.

5.5 HYPOTHALAMIC SRPX2 EXPRESSION REMAINS UNALTERED AFTER CCI-INDUCED TBI IN MICE (II)

Next, the effect of acquired brain injury on SRPX2 expression was investigated in wild type, *Plaur*$^{-/-}$ and *Plau*$^{-/-}$ mice exposed to CCI-induced TBI.

SRPX2-ir neuronal numbers in the hypothalamus of naïve, sham and CCI-injured Wt mice were compared. SRPX2-ir neurons were distributed in Pa, Pe and SO nuclei and no difference was observed in SRPX2-ir neuronal counts between naïve and sham-operated animals. Stereological cell counting revealed that the total number of SRPX2-ir neurons in ipsilateral Pa (1057 ± 178 vs. 976 ± 104), Pe (392 ± 24 vs. 318 ± 46) and SO (507 ± 45 vs. 478 ± 72) nuclei did not change in mice at 4 d post-TBI when compared to the control group (naïve and sham pooled together) ($p>0.05$). No difference was observed in the hypothalamic SRPX2-ir neuronal counts between the ipsilateral and contralateral sides in the TBI or control groups ($p>0.05$) **(II, Fig. 3)**. *Srpx2* gene expression in hypothalamus, perilesional cortex, hippocampus and thalamus did not differ between Wt-sham and Wt-CCI mice at 4 d and 14 d post-TBI ($p>0.05$) **(II, Fig. 4)**.

The effect of genotype and acquired brain injury on *Srpx2* gene expression in the hypothalamus, perilesional cortex, hippocampus and thalamus was investigated at 4 d and 14 d post-TBI **(II, Fig. 4)**. *Srpx2* gene expression in the hypothalamus, hippocampus and thalamus did not differ between injured Wt, *Plaur*$^{-/-}$ and *Plau*$^{-/-}$ mice at 4 d and 14 d post-CCI ($p>0.05$). However, *Srpx2* gene expression was higher in the perilesional cortex of the *Plau*$^{-/-}$-CCI group at 4 d post-TBI as compared to sham-operated controls ($p<0.05$). No difference was observed in gene expression of *Srpx2* in *Plaur*$^{-/-}$-CCI mice at 4 d post-TBI compared with sham-operated animals ($p>0.05$) **(II, Fig. 4)**. At 14 d post-TBI, *Srpx2* gene expression did not differ between the CCI and sham groups in any of the genotypes **(II, Fig. 4)**. Unsupervised hierarchical clustering utilizing *Srpx2* gene expression did not identify any unique clusters based on genotype, injury or time after injury **(II, Fig. 7)**.

Taken together, SRPX2 protein and *Srpx2* gene expression in Wt mice after CCI was comparable to naïve and sham Wt mice. Furthermore, no effect of genotype or injury was observed on hypothalamic *Srpx2* gene expression in knockout mice. However, *Srpx2* gene expression was upregulated in cortex of Plau$^{-/-}$-CCI mice 4 days after CCI.

5.6 CCI DIFFERENTIALLY REGULATES UPAR AND UPA GENE EXPRESSION IN MICE (II)

The SRPX2 expression in Wt and knockout mice did not suggest any robust genotype or injury-related effects on SRPX2-ir neuronal numbers or mRNA. Therefore, it was assessed whether the other components of uPAR-interactome were also resistant to genetic and acquired lesions. Ipsilateral and contralateral hypothalamus, perilesional cortex, hippocampus and thalamus were analysed from sham-operated (Wt-Sham, *Plaur*$^{-/-}$-Sham and *Plau*$^{-/-}$-Sham) and CCI-injured animals (Wt-CCI, *Plaur*$^{-/-}$-CCI and *Plau*$^{-/-}$-CCI) at 4 d and 14 d after TBI, and the gene expression of *Plau* and *Plaur* was analyzed using RT-qPCR **(II, Fig. 5-6)**. In naïve Wt, *Plaur*$^{-/-}$ and *Plau*$^{-/-}$ mice, *Plau* and *Plaur* gene expression in hypothalamus, cortex, hippocampus and thalamus did not differ between the genotypes.

After CCI-induced TBI, hypothalamic gene expression of *Plau* and *Plaur* did not differ in Wt-CCI, *Plaur*$^{-/-}$-CCI and *Plau*$^{-/-}$-CCI mice compared with respective sham mice at 4 d and 14 d post-TBI ($p>0.05$). However at 4 d and 14 d post-TBI, gene expression of *Plau and Plaur* was increased in the ipsilateral perilesional cortex, hippocampus and thalamus of Wt-CCI, *Plaur*$^{-/-}$-CCI and *Plau*$^{-/-}$-CCI mice compared with respective sham mice ($p<0.05$) **(II, Fig. 5-6)**.

When unsupervised hierarchical clustering was applied on gene expression data, *Plaur* and *Plau* gene expression differentiated mice into two main clusters, sham and injured, irrespective of the time after injury indicating an injury effect on *Plaur* and *Plau* gene expression irrespective of genotype **(II, Fig. 7)**.

Taken together, CCI-induced TBI differentially regulates Plau and Plaur gene expression in cortex, hippocampus and thalamus. Plau and Plaur gene expression in hypothalamus remains unaltered after CCI-induced TBI.

5.7 SRPX2 EXPRESSION IS DOWNREGULATED ACUTELY AFTER FPI (III)

Next, a comprehensive study investigating spatiotemporal expression of SRPX2 in rat brain and plasma was done in an another experimental model of TBI. Lateral FPI-induced injury was induced in rats and SRPX2 expression in brain and plasma was evaluated at 2 h, 6 h, 24 h, 48 h, 72 h, 5 d, 7 d, 14 d, 1 month and 3 months post-lateral FPI **(III, Fig. 1)**.

5.7.1 SRPX2 expression in plasma after lateral FPI (III)

Western blot analysis identified differential expression of SRPX2 in plasma. For better readability, post-TBI time points are presented here as groups including acute (2 h, 6 h, 24 h), sub-acute (48 h, 72 h, 5 d, 7 d, 14 d) and chronic (1 month, 3 months) **(III, Fig. 2)**.

At 2 h post-TBI, a marked decrease in the SRPX2 levels in plasma was observed as compared to sham-operated experimental controls (12.50 ± 5 vs 51.6 ± 3.18, $p<0.01$) and naïve group (12.5 ± 5 vs 78.8 ± 13.4, $p<0.01$) **(III, Fig. 2)**. ROC analysis identified that plasma SRPX2 levels at 2 h post-TBI can differentiate between injured and sham-operated experimental control (AUC= 1.00, $p<0.05$), and between injured and naïve rats (AUC=1.00, $p<0.05$) **(III, Fig. 3)**.

At 6 h post-TBI, the plasma SRPX2 levels started to recover and the plasma SRPX2 levels at 6 h-24 h post-TBI (46.83 ± 5.8) were higher than 2 h post-TBI (12.50 ± 5, $p<0.01$) **(III, Fig. 2)**. Between 48 h and 14 d post-TBI, the plasma SRPX2 levels were higher than 2 h post-TBI (43.76 ± 6.8 vs 12.50 ± 5, $p<0.005$). The plasma SRPX2 levels were highly variable during this post-injury time window **(III, Fig. 2)**.

At 1-3 months post-TBI, the SRPX2 levels in plasma had recovered completely and were not different from those detected in the naïve group (78.64 ± 14.2 vs 78.89 ± 13.4, $p>0.05$) **(III, Fig. 2)**.

The SRPX2 plasma levels did not correlate with body weight, impact severity or the duration of the post-impact apnea.

5.7.2 Hypothalamic SRPX2-ir neurons after lateral FPI (III)

In view of the downregulation of SRPX2 plasma levels at 2 h post-TBI, SRPX2 expression in brain was investigated to evaluate if the changes in plasma SRPX2 expression correlated with that of the brain. Quantitative estimation of number of SRPX2-ir neurons in rat hypothalamus was done at 2 h, 6 h, 24 h, 48 h, 24 h, 48 h, 72 h, 5 d, 7 d, 14 d and 1 month post-TBI **(III, Fig. 4)**.

At 2 h post-TBI, a reduction in the total number of SRPX2-ir neurons in hypothalamic Pa (2076 ± 386 vs 4344 ± 247, $p<0.05$) and SO (2468 ± 202 vs 4532 ± 419, $p<0.05$) nuclei was observed as compared with the naïve group. Together, the total number of SRPX2-ir neurons in the hypothalamus at 2 h post-TBI (5032 ± 527 vs 9440 ± 351) was 53% of that in the naïve rats. The number of SRPX2-ir neurons in sham-operated experimental controls was not different from the naïve group ($p>0.05$). At 6 h post-TBI, SRPX2-ir neuronal numbers were 84% and 78% of that in naive Pa and SO nuclei, respectively. The total number of SRPX2-ir neurons in the hypothalamus was comparable between naïve and 24 h post-TBI (99% of naïve) **(III, Fig. 4)**. A decrease in SRPX2-ir neurons was also seen at 48 h post-TBI lasting up to 14 d post-TBI. During this time window, SRPX2 expression varied between animals of the same time point **(III, Fig. 4)**. At 1 month post-TBI, the number of SRPX2-ir neurons in the hypothalamus was 97% of the naïve rats ($p>0.05$) **(III, Fig. 4)**. Further analysis showed no significant correlation between total number of SRPX2-ir neurons in hypothalamus after TBI and body weight, impact severity or post-impact apnea.

In depth analysis of the decrease in hypothalamic SRPX2-ir neuronal counts at 2 h post-TBI showed that the downregulation was bilateral. Within the Pa nucleus, it was more pronounced in neurons of the dorsal cap of Pa (PaDC), lateral magnocellular Pa (PaLM), medial parvocellular Pa (PaMP) and ventral part of Pa (PaV) (bregma level -1.80 to -1.92 mm). The numbers of SRPX2-ir neurons in the anterior parvocellular Pa (PaAP), medial magnocellular Pa (PaMM) (bregma level -0.96 to -1.60 mm) and posterior Pa (PaPo) (bregma level -2.04 mm) were comparable between the naïve and 2 h post-TBI groups ($p>0.05$) **(III, Fig 5)**. The cytoplasmic SRPX2 protein has a granular appearance under higher magnification. The number of SRPX2-ir granules per SRPX2+ neuron between the naïve and 2 h post-TBI group were counted. The number of SRPX2-ir granules/cell in the ipsilateral Pa at 2 h post-injury was reduced (62.9 ± 2.6 vs 71.3 ± 3.5, $p<0.05$) as compared with the naïve group **(III, Fig. 6)**. SRPX2-ir fibers from the Pa and SO neurons travel ventrally towards the hypophysis. The density of SRPX2-ir fibers on the ipsilateral side of the hypothalamus of the injured rats did not differ from that on

the contralateral side (37.8 ± 11.8 vs 34.6 ± 7.7, p>0.05). Moreover, the mean ipsilateral SRPX2-ir fiber density at 2 h post-TBI (37.8 ± 11.8 vs 53.3 ± 12.5, p>0.05) was comparable with that of the naive group **(III, Fig. 6)**.

5.7.3 FPI-induced SRPX2 expression in plasma correlates with brain (III)

Overall, the plasma SRPX2 levels correlated with hypothalamic SRPX2-ir neuronal numbers when all post-TBI time points were pooled together (r=0.46, p<0.05) **(III, Fig 7A)**. However, when analysed individually, the plasma SRPX2 levels did not correlate with SRPX2-ir neuronal numbers in hypothalamus at the sub-acute time points. At 2 h and 1 month post-TBI, the number of SRPX2-ir neurons in hypothalamus strongly correlated with the plasma SRPX2 level from the same animals (r=0.89, p<0.001 and r=0.94, p<0.001) **(III, Fig. 7)**.

Unsupervised hierarchical clustering was applied to the SRPX2 protein expression data obtained by western blot and immunohistochemistry to investigate whether animals can be clustered into groups based on the number of SRPX2-ir neurons in the Pa, Pe, SO and hypothalamus or the plasma SRPX2 levels. No assumptions were made in the clustering analysis (hence, unsupervised) and thus the analysis determined the relatedness of cases based on the pattern of SRPX2 protein expression irrespective of the experimental group.

Two main clusters were identified based on the number of SRPX2-ir neurons in Pa, Pe and SO nuclei, where cluster 1 included 2 h, 6 h, 72 h, 5 d, 7 d and 14 d post-TBI groups. Cluster 2 contained 24 h, 48 h and 1 month post-TBI groups in addition to the naïve and sham groups indicating that hypothalamic SRPX2 protein expression at 24 h, 48 h and 1 month post-TBI is comparable with the control groups **(III, Fig 8)**. Similarly, unsupervised hierarchical clustering based on the plasma SRPX2 levels and number of SRPX2-ir neurons in hypothalamus identified two main clusters. Cluster 1 comprised of the 2 h, 6 h, 72 h, 5 d, 7 d and 14 d groups and cluster 2 grouped the 24 h, 48 h and 1 month post-TBI groups together with naïve and sham-operated experimental control animals **(III, Fig 8)**.The unsupervised hierarchial clustering analysis indicated that SRPX2 expression is differentially regulated in rats after lateral FPI. However, the clustering of 24-h, 48-h, and 1-month post-TBI groups with control groups indicated that the SRPX2 expression in the brain and plasma at these time points was comparable between controls and TBI.

5.7.4 Hypothalamic oxytocin-ir neurons after lateral FPI (III)

In order to investigate whether the reduction in the number of SRPX2-ir neurons correlates with number of oxytocin-ir neurons in hypothalamus, oxytocin immunolabeling was done in naïve and 2 h post-TBI group. Like SRPX2, the total number of hypothalamic oxytocin-ir neurons decreased at 2 h post-TBI as compared to the naïve group (4780 ± 794 vs 8408 ± 278, p<0.001). Moreover, the number of oxytocin-

ir neurons in the hypothalamus correlated strongly with the number of SRPX2+ neurons ($r=0.99$, $p<0.01$) in the same animals at 2 h post-TBI **(III, Fig. 10)**.

Overall, these data indicate that lateral FPI leads to hypothalamic injury. Furthermore, an injury-specific downregulation of SRPX2 expression is observed after lateral FPI and it can be proposed that SRPX2 protein may serve as a candidate biomarker of hypothalamic injury.

5.8 LATERAL FPI LEADS TO REDUCTION IN NEUROHYPOPHYSEAL VOLUME (IV)

MRI studies have previously demonstrated that the rat hypophysis has an irregular shape and is located on the ventral side of the brain (Theunissen et al., 2010). The outer margins of hypophysis in mid-sagittal and coronal planes were identifiable using MRI but individual lobes could not be distinguished. Using MEMRI, the three lobes of the rat hypophysis (adenohypophysis, intermediate lobe, neurohypophysis) were identified and located distinctively in the coronal plane as previously shown (Silva et al., 2004) **(IV, Fig. 1).**

First, the total hypophyseal volume was estimated in the sagittal plane from structural MRI images of animals scanned at 2 d and 5 months post-TBI. The total hypophyseal volume did not change in the injured group at 2 d post-TBI (10.49 ± 0.23 mm^3 vs 10.32 ± 0.50 mm^3) or 5 months post-TBI (10.66 ± 0.43 mm^3 vs 11.28 ± 0.87 mm^3) when compared to sham-operated animals **(IV, Fig. 2)**.

Next, the total hypophyseal volume was estimated in coronal MEMRI images at 8 months post-TBI. The total volume of the hypophysis in the injured group (12.30 ± 0.43 mm^3 vs 12.25 ± 0.46 mm^3) was not different when compared to sham-operated animals. Taken together, the total volume of the hypophysis in the injured group did not differ between 2 d, 5 months and 8 months post-TBI **(IV, Fig. 3)**.

In order to identify TBI-induced volumetric changes in both lobes of hypophysis separately, MEMRI images were used to estimate the volume of the adenohypophysis and neurohypophysis in sham and injured animals at 8 months post-TBI. The adenohypophysis volume was not different between the TBI and sham-operated controls (11.32 ± 0.4 mm^3 vs 11.22 ± 0.45 mm^3). Interestingly, neurohypophyseal volume was reduced in TBI group as compared to sham-operated control group (1.04 ± 0.05 mm^3 vs 1.25 ± 0.05 mm^3, $p<0.05$). Similar total hypophyseal volumes were obtained by volumetric analysis of MEMRI images in sagittal and coronal planes (12.35 ± 0.40 mm^3 vs 12.29 ± 0.43 mm^3, $p>0.05$) at 8 months post-TBI, and the volumes correlated with each other ($r=0.97$, $p<0.05$) **(IV, Fig. 3)**.

5.9 NEUROHYPOPHYSEAL VOLUME CORRELATES WITH SEIZURE SUSCEPTIBILITY AND IMPAIRED SPATIAL LEARNING (IV)

In order to investigate whether hypophyseal atropy associates with functional outcome after TBI, correlation of hypophyseal, neurohypophyseal and adenohypophyseal volumes with the outcome in the PTZ and Morris water-maze tests were analyzed. The analysis showed that the smaller the hypophyseal volume, the shorter the time to the first PTZ-induced epileptiform discharge post-TBI ($r=0.632$, $p<0.05$). The smaller the neurohypophyseal volume, the greater the total number of PTZ-induced epileptiform discharges ($r=-0.796$, $p<0.05$). Furthermore, the smaller the neurohypophyseal volume, the longer the mean latency to platform ($r=-0.629$, $p<0.05$) and mean path distance travelled ($r=-0,621$, $p<0.05$) in the Morris water-maze **(IV, Fig. 4)**.

5.10 SUMMARY OF RESULTS

Overall, study I-IV demonstrated that SRPX2 is expressed in brain and SRPX2 expression in hypothalamus is regulated independent of uPAR interactome. Lateral FPI differentially regulates SRPX2 expression and leads to structural atrophy in hypophysis (Table 5).

Table 5. Summary of results obtained in study I-IV.

Study	Main findings
I	SRPX2 protein is expressed in hypothalamus and this expression is highly conserved between mouse, rat, monkey and human brain. SRPX2 protein colocalizes with oxytocin or vasopressin in the Pa and SO nuclei. SRPX2-ir fibres project to the hypophysis and brain stem. SRPX2 protein is present in plasma and CSF.
II	SRPX2 expression in mouse hypothalamus is unaffected by the deficiency of uPAR and uPA with or without acquired brain injury. *Plau* and *Plaur* gene expression in hypothalamus of Wt and knock out mice remains unaltered after CCI-induced TBI. The expression of uPAR and uPA in cortex, thalamus and hippocampus is regulated by genetic and acquired lesions.
III	SRPX2 protein expression is acutely reduced after lateral FPI in rats. The decrease in plasma SRPX2 levels correlate with the number of SRPX2-ir neurons in the hypothalamus. The number of oxytocin-ir neurons also decrease bilaterally 2 hours after TBI indicating FPI-induced hypothalamic damage.
IV	Lateral FPI results in reduction of neurohypophyseal volume in rats 8 months after injury. The hypophyseal volume corelates with increased siezure susceptibility and impaired spatial learning.

6 DISCUSSION

The aim of this thesis was first to investigate the expression of SRPX2 in normal brain and to identify if this expression is modulated by the SRPX2-uPAR interaction. The second part of the thesis focused on studying the effect of acquired brain injury on hypothalamo-pituitary axis, particularly exploring the changes in SRPX2 expression in brain and plasma after TBI. Furthermore, it was investigated whether experimental traumatic brain injury recapitulated human injury-induced hypophyseal atrophy.

The results presented in this thesis demonstrated the following: first, SRPX2 protein is expressed in the Pa, Pe, and SO nuclei of the mouse, rat, monkey, and human hypothalamus, and SRPX2-ir projections travel to the neurohypophysis and brainstem. SRPX2 protein colocalized with oxytocin or vasopressin, and SRPX2 protein is present in rat and human plasma, as well as in human CSF. Second, the genetic deficiency of uPAR and uPA did not affect SRPX2 expression in hypothalamus, and CCI-induced TBI did not regulate hypothalamic SRPX2 expression when assessed at acute and sub-acute post-TBI phase. Thirdly, it was observed that lateral FPI-induced TBI leads to acute downregulation of SRPX2 protein in the hypothalamus and plasma, consequently identifying SRPX2 as a candidate biomarker of hypothalamic injury. Lastly, it was found that lateral FPI-induced TBI also leads to structural changes in hypophysis, resulting in decreased neurohypophyseal volume at chronic post-injury time point, and the neurohypophyseal volume correlated with increased seizure susceptibility and poor memory and spatial learning.

6.1 METHODOLOGICAL CONSIDERATIONS

6.1.1 Human brain tissue

Postmortem human brain tissue was used in this study. While brain tissue obtained by autopsy serves as an important resource for understanding the diseases of the nervous system, several factors can affect the tissue and molecular preservation of these samples (Ferrer et al., 2008). For example, postmortem delay, storage temperature and procedures of tissue preservation can introduce variations in DNA, RNA and protein profile of the tissue. Additionally, pre-mortem events like prolonged agonal state, hypoxia, acidosis, fever and seizures may also influence the data obtained. In this study, only cases without a known neuronal pathology were included. The processing time and procedure was comparable and standardized.

6.1.2 Animal models

Two experimental models of TBI, including CCI and lateral FPI, were used in this study. Both CCI and lateral FPI are well-characterized and highly reproducible models

of TBI (McIntosh et al., 1989b; Smith et al., 1995). While animal models provide an opportunity to understand the underlying pathophysiology of human TBI, there is still a large translational gap between rodent and human studies because of the pathophysiological heterogeneity in patients with TBI arising due to location, nature and severity of primary injury.

Two knockout mouse models (*Plaur*$^{-/-}$ and *Plau*$^{-/-}$) were used in this thesis. For both *Plaur*$^{-/-}$ and *Plau*$^{-/-}$, Wt littermates were used as controls. In view of previous reports on reduction of γ-aminobutyric acid (GABA) expressing cortical neurons in *Plaur*-deficient mice at the age of P20 (Eagleson et al., 2005), the counting of SRPX2-ir neurons in hypothalamus of *Plaur*$^{-/-}$ and *Plau*$^{-/-}$ mice was done in P20 mice to maximize the chance of identifying the effect of *Plaur* deficiency on SRPX2 expression. However, no difference was seen in SRPX2+ neuronal numbers between P20 and adult mice.

6.1.3 Gender effect

Sexual dimorphism in gene expression has been well documented (Trabzuni et al., 2013). In this study, human brain tissue, hypophysis, CSF and blood samples were acquired from both male and female cases. SRPX2 expression was observed in both genders. It is however beyond the scope of the current study to unequivocallt rule out differences in SRPX2 expression due to the potential genetic variability in the human cases studied. All experiments in rodents were carried out in male mice and rats. Therefore, further studies in rodents will be needed to address gender-based differences in SRPX2 expression after TBI.

6.1.4 RNA analysis

RT-qPCR is a well-established method for quantification of RNA from blood and brain tissue. However, the choice of housekeeping gene is a crucial step in normalization and interpretation of data (Kozera and Rapacz, 2013). In this study, two housekeeping genes, *Gapdh* and *ACTB*, were used for normalization of RT-qPCR data. The housekeeping gene expression did not change between the control and diseased group. For *in situ* hybridization, negative control assays were run in parallel to the experimental assays. The specificity of the probe was determined using the *in silico* probe designing tools.

6.1.5 Immunological methods

Antibodies are the most commonly used research tools and antibody validation is central to the reproducibility of research data. This thesis relies heavily on the use of antibodies for investigation of SRPX2 expression in rodent and human samples. Therefore, the specificity of the antibody was evaluated using the approaches proposed by the International Working Group for Antibody Validation (Uhlen et al., 2016). Using siRNA based silencing, the specificity of SRPX2 antibody was determined and the same

antibody was used in immunohistochemistry and western blot analysis. The reproducibility of the results was also confirmed using another antibody against SRPX2 which detects a different epitope on the SRPX2 protein. However, it is important to realize that the current antibody might not detect SRPX2 protein with potential disease-specific post-translational modifications.

6.1.6 Western blot

Western blot was used in this study to detect plasma SRPX2 levels. Western blot quantification depends on the densitometry of the immunopositive band which may be affected by factors like the protein load, incomplete protein transfer and saturation of the signal. Therefore, appropriate control experiments were done to ensure reproducibility of the data. Dilution series of samples were run to determine the linearity of detection. Densitometry was done by drawing region of interest manually. Furthermore, owing to the variable expression of commonly known housekeeping proteins, total protein was used for normalization. It is important to appreciate the fact that western blot offers relative quantification only. To measure the plasma SRPX2 levels in a more robust and precise way, methods like enzyme-linked immunosorbent assay (ELISA) should be employed. In this study, commercially available SRPX2 ELISA kits for rats were tested but were not used eventually due to their non-linear detection of SRPX2 protein.

6.2 SRPX2 EXPRESSION IN NORMAL BRAIN

SRPX2 expression was first identified in leukemia cells with an E2A-HLF fusion protein (Kurosawa et al., 1999). Later, mutations in human *SRPX2* gene were found to be associated with Rolandic epilepsy, mental retardation, and speech dyspraxia (Roll et al., 2006, 2010; Sia et al., 2013). Further studies reported SRPX2 expression in cortex, and found that *in utero* silencing of *Srpx2* led to impaired vocalizations and epileptiform activity in mouse pups (Roll et al., 2006; GM et al., 2013). Despite these reports on potential role of SRPX2 in brain pathology, the spatial and cellular localalization of SRPX2 in brain was not identified.

In the first part of this thesis, SRPX2 expression was characterized in normal brain. It was also investigated whether SRPX2 expression in brain is phylogenetically conserved. Interestingly, SRPX2 expression was found in hypothalamic nuclei instead of the ultrasonic vocalization related temporal cortex in mice and rats. Strong SRPX2 immunoreactivty was observed in the neurons of paraventricular, periventricular and supraoptic nuclei, and SRPX2 immunoreactive fibers were identified in the brain stem and hypophysis. These findings were consistent in rat, mouse, monkey and human brain indicating a highly conserved expression of SRPX2 in brain.

Contrary to previous reports, no immunoreactivity was found in cortex. A stringent antibody validation strategy was employed to verify these findings. siRNA based gene silencing was carried out *in vitro*, and multiple tissue processing and histological strategies were employed. In addition to the validated antibody, all the immunostainings were repeated using a monoclonal anti-SRPX2 antibody. Studies by Roll *et al* reported SRPX2 immunostaining in rat and human cortex using an in-house antibody (Roll et al., 2006)). This in-house antibody (generously provided by Professor P Szepetowski) was also used for immunostaining of rat and human brain tissue using protocol by Roll *et al* and the protocol used in the current study. However, none of these approaches showed any distinct SRPX2 immunoreactivity in the cortex whereas hypothalamic staining was consistently detected in all types of staining strategies. The difference in SRPX2 immunodetection in cortex can be due to differential post-translational modifications of SRPX2 protein, unidentified SRPX2 protein variants or variable epitope recognition by anti-SRPX2 antibodies (Tanaka et al., 2012). It is, however, still to be investigated whether SRPX2 protein expression in cortex is conditionally regulated in different brain pathologies.

In the current study, SRPX2-ir neurons were located in the hypothalamic Pa nucleus. The Pa nucleus plays a central role in mediating the physiological functions of the hypothalamus (Swanson and Sawchenko, 1983). It has a functionally distinct type of neurons including the neurosecretory magnocellular neurons, the neuroendocrine parvocellular neurons and the pre-autonomic parvocellular neurons projecting to the posterior pituitary, the median eminence, and the nucleus tractus solitarius, rostral ventrolateral medulla, and spinal cord, respectively (Swanson and Sawchenko, 1983; Ferguson et al., 2008; Loewen et al., 2017). The observed topographic organization of SRPX2-ir projections to the hypophysis and brainstem was in line with these well-characterized projections. Further studies are needed to investigate the functional connectivity of SRPX2-ir fibers in brain.

The study also provided the first evidence for the presence of SRPX2 protein in plasma and CSF. Using western blot, SRPX2 immunoreactive band was detected in rat and human plasma. SRPX2 protein was also detected in human CSF. These observations indicated that SRPX2 is detectable in blood, and may serve as a target for non-invase biomarker discovery.

The colocalization of SRPX2 protein with oxytocin or vasopressin in the Pa and SO nuclei suggested a role of SRPX2 protein in neuroendocrine functions. However, it is yet to be explored whether SRPX2 expression in hypothalamus can contribute to development of language. Few studies have associated oxytocin levels with with social communication, vocal learning and language in humans (Pfundmair et al., 2016; Ye et al., 2016; Zhang et al., 2016; Theofanopoulou et al., 2017). It was further shown that oxytocin knockout mice exhibit reduced ultrasonic vocalizations (Winslow et al., 2000). These data together with the findings of this thesis suggest that the expression of SRPX2 protein in the hypothalamus may have an indirect impact on social behavior and communication.

6.3 SRPX2 AND THE UPAR INTERACTOME

The ECM plays a central role in post-injury tissue remodelling and alleviation of evolution of co-morbidities, and thus serves as a rich source of novel treatment targets (Soleman et al., 2013).SRPX2 has been recently identified as a novel ligand of uPAR which is an essential component of the ECM fibrinolytic machinery. uPAR, along with its other ligand, uPA, have been shown to play an important role in trauma, epilepsy and language impairment among other brain disorders (Masos and Miskin, 1997; Lahtinen et al., 2006b, 2009; Royer-Zemmour et al., 2008a; Roll et al., 2010; Iyer et al., 2010; Liu et al., 2010; Bruneau and Szepetowski, 2011; Eden et al., 2011; Quirico-Santos et al., 2013; Rantala et al., 2015; Bolkvadze et al., 2016). Despite the initial reports of SRPX2-uPAR interaction (Royer-Zemmour et al., 2008b), very little is known about the role of uPAR interactome in the regulation of SRPX2. Therefore, as a first step to understand the factors that regulate SRPX2, the current study investigated if the genetic deficiency of uPAR or its ligand uPA affects SRPX2 expression.

Similar to the wild type mice, SRPX2 expressing neurons were localized in hypothalamic Pa, Pe and SO nuclei of uPAR and uPA-deficient mice, and no immunoreactivity was detected in the cortex. The total number of hypothalamic SRPX2 immunoreactive neurons were also comparable between wild type, uPAR and uPA-deficient mice, suggesting uPAR interactome independent regulation of hypothalamic SRPX2 expression.

uPAR has been shown to regulate brain plasticity during development and after brain damage (Lahtinen et al., 2006b; Liu et al., 2010; Smith and Marshall, 2010; Archinti et al., 2011; Quirico-Santos et al., 2013). A deficiency in uPAR encoding gene, *Plaur*, resulted in a severe epilepsy phenotype after intrahippocampal kainate injection (Ndode-Ekane and Pitkänen, 2013). Taken together, uPAR plays an important role in the post-injury outcome but the underlying molecular interactions are still not fully understood. Therefore, the current study investigated if SRPX2 expression in wild type, uPAR and uPA-deficient mice would be differentially regulated after traumatic brain injury. TBI was induced using CCI, which is an extensively used animal model of a closed head injury that recapitulates many of the behavioral, anatomical and functional aspects of human TBI (Statler et al., 2008; Statler et al., 2009; Hunt et al., 2009; Hunt et al., 2010; Hunt et al., 2011; Bolkvadze and Pitkänen, 2012; Hunt et al., 2012).

The SRPX2 gene and protein expression remained unaltered in the hypothalamus of wild type, uPAR and uPA-deficient mice after CCI. However, *Srpx2* gene expression was upregulated in the ipsilateral perilesional cortex of uPA-deficient mice at 4 d post-CCI, and returned to control levels at 14 d post-TBI, reflecting the acute response to injury. No difference was observed in cortical *Srpx2* gene expression in wild type and uPAR-deficient mice after CCI indicative of a genotype-specific effect on SRPX2 expression in uPA-deficient mice. These observations further suggest that the augmented availability of uPAR receptor, and the deficiency of its functional ligand,

uPA, may induce an acute compensatory upregulation of *Srpx2* gene expression at the lesion site.

Unlike SRPX2, the expression of both uPAR and uPA were differentially regulated by CCI-induced acquired brain injury. Furthermore, unsupervised hierarchical clustering, using uPA and uPAR gene expression, clustered mice into sham and injured groups irrespective of the time after injury. These observations are consistent with previous reports indicating increased expression of uPAR and uPA in brain injury and epilepsy (Beschorner et al., 2000; Lahtinen et al., 2006b, 2009; Ndode-Ekane and Pitkänen, 2013). For instance, the number of uPAR+ cells increased in the perilesional cortex at 4 d after TBI in humans (Beschorner et al., 2000). Further studies are, however, needed to identify post-TBI changes in uPAR and uPA protein expression in this experimental model of TBI.

Taken together, the above data indicated uPAR-interactome independent role of SRPX2 expression in the hypothalamus, which however does not exclude its potential role in TBI-induced comorbidities. The gene expression of *Srpx2* in the perilesional cortex of uPA deficient mice suggests its role in uPAR-mediated tissue remodeling after TBI. The expression of uPAR and uPA is regulated by genetic and acquired lesions.

6.4 SRPX2 EXPRESSION AFTER TRAUMATIC BRAIN INJURY

SRPX2 expression in hypothalamus did not change in mice at 4 and 14 days after CCI-induced TBI. Therefore, a more detailed investigation was conducted to investigate the TBI-induced spatiotemporal changes in SRPX2 protein expression in brain at acute and chronic time points after injury. Plasma SRPX2 levels were also investigated to explore the potential of SRPX2 as a biomarker of injury. The lateral fluid-percussion injury model of TBI was used to maximize the possibility of detecting the subcortical damage in addition to cortical pathology.

In this study, an acute reduction in plasma SRPX2 levels was observed at 2 h post-TBI, and the plasma SRPX2 levels correlated with the number of SRPX2-ir neurons in the hypothalamus, indicating a potential brain-specific regulation of SRPX2 after TBI. Between 6 h post-FPI and 14 d post-FPI, the expression of SRPX2 was variable in plasma and brain and did not correlate with each other in all cases. This variable SRPX2 expression during the first two weeks of injury can be attributed to the ongoing injury-induced cellular and molecular processes (Pitkänen et al., 2018). The brain and plasma SRPX2 expression recovered within 1 month post-LFPI and was compareable with controls.

The number of SRPX2-ir neurons in the hypothalamus decreased bilateraly at 2 h post-TBI with the decrease being was most visible in the Pa nucleus. Damage to the hypothalamic Pa has been documented previously in the lateral FPI model of TBI (Roe et al., 1998). For example, a bilateral upregulation in corticotropin-releasing hormone (CRH) mRNA was observed in the hypothalamic Pa at 2 hours post-FPI (Roe et al., 1998)

Furthermore, post-traumatic hyperthermia in rats 7 days after LFPI was associated with increased astrocytosis and inflammation in hypothalamic Pa (Thompson et al., 2005a).

In humans, a hypothalamic injury is not uncommon and has lead to dysfunctional hypothalamic connectivity after TBI (Baumann et al., 2009; Zhou, 2017). However, the lack of hypothalamic injury-specific biomarkers limit the detection and progression of TBI-induced endocrinopathy. The current study indicated that the hypothalamus is vulnerable to TBI-induced damage and the lateral FPI model of TBI recapitulates hypothalamic injury in humans. Furthermore, in light of SRPX2 expression in the hypothalamus, and alteration in its brain and plasma levels after TBI, it can be proposed that SRPX2 protein plays a role in modulating the post-traumatic outcome and that plasma SRPX2 levels can serve as a biomarker of hypothalamic injury. Taken together, these observations widen avenues for novel therapeutic strategies for treating TBI-associated pathology and comorbidities.

6.5 SRPX2 AS A BIOMARKER OF HYPOTHALAMIC INJURY AFTER TBI

SRPX2 protein is a novel protein and have been associated with Rolandic epilepsy in humans. However, there are no studies in rodents or humans investigating the expression of SRPX2 after TBI. In the current study, changes in SRPX2 expression were investigated in two experimental models of TBI including CCI and lateral FPI. While both models mimic various aspects of human TBI, some aspects are unique to each one of them. For instance, CCI results in a focal cortical injury wheras lateral FPI results in a diffused cortical and sub-cortical injury. The current study reports acute downregulation of SRPX2 expression in brain and plasma after lateral FPI. However, no effect of CCI-induced TBI on SRPX2 protein and mRNA levels was found. The difference in these observations can be due to the various factors. For instance, lateral FPI lead to hypothalamic injury and consequently altered SRPX2 expression wheras CCI-induced injury was mainly localized to cortex, thalamus and hippocampus indicating a more focal cortical injury in CCI. Like SRPX2, uPAR and uPA expression in hypothalamus also remained unaltered. Secondly, CCI-induced alterations in SRPX2 expression were investigated at 4 day and 14 days post-TBI based on previous observations from studies in uPAR and uPA-deficient mice. However, the lateral FPI-induced reduction in SRPX2 expression was detectable at 2 hours post-injury. Similar to CCI, SRPX2 expression at 4 day and 14 days post-FPI was comparable to controls. However, it is still to be explored whether SRPX2 expression is reduced 2 hours post-CCI. Lastly, wild type and knock out mice were used in the CCI study whereas rats were used in lateral FPI due to their respective ease of operation and low mortality rates (Johnson et al., 2015). Therefore, the current study does not rule out the effect of species on TBI-induced changes in SRPX2 expression. Despite the aforementioned limitations, these findings provide novel

observations and open new venues for investigating hypothalamic damage and TBI-associated co-morbidities

6.6 HYPOTHALAMO-PITUITARY AXIS IN TBI

The first three studies presented in this thesis established the expression of SRPX2 in hypothalamus and hypophysis, and that a lateral FPI-induced injury altered SRPX2 expression. Finally, it was investigated whether lateral FPI-induced injury could cause a structural pathology in the hypothalamo-pituitary axis.

The hypothalamus-pituitary axis regulates endocrine and autonomic functions which are necessary for survival in both rodents and humans. An injury to the hypothalamus may lead to chronic pituitary dysfunction (Tanriverdi et al., 2015). For example, water balance in body is regulated by vasopressin-expressing neurons in hypothalamus and TBI can lead to their dysregulation causing diabetes insipidus (Capatina et al., 2015). The etiology of post-TBI pituitary dysfunctions still remains to be clarified. However, the confinement of the pituitary gland in the sella turcica makes it vulnerable to damage due to the rotational and shearing forces caused by mechanical trauma (Dusick et al., 2012).

In this study, MRI was used to measure the volume of hypophysis at acute and chronic time points (2 d and 5 months) after lateral FPI-induced injury. No difference was observed between the volume of hypophysis between controls and TBI groups. Previously, a retrospective MRI study in patients with TBI showed an increased hypophyseal volume acutely (<7 days post-injury) that normalized over time (8-15 months post-injury) (Maiya et al., 2008). This difference in observation can be attributed to the heterogeneous nature of injury in humans.

MRI identified the boundaries of hypophysis in sagittal plane but could not delineate the two lobes separately. Therefore, MEMRI was utilized to distinctly identify the boundaries of adenohypophysis and neurohypophysis. Consequently, a reduction in the volume of the neurohypophysis was observed at 8 months after lateral FPI. Interestingly, the effect of injury could only be detected when the volume of each lobe was investigated seperatly and not as total volume. It can be suggested that the change in the neurohypophyseal volume is masked in the total hypophyseal volume and not detectable due to the relatively large size of the adenohypophysis.

It was also noted that TBI animals with a small total hypophyseal volume had a shortened delay to the first PTZ-induced epileptiform discharge. An increased number of epileptoform discharges after PTZ injection was observed in the rats with a small neurohypophyseal volume. These findings suggest that hypophyseal damage is associated with increased seizure susceptibility. Previous studies have reported an association of abnormal neuroendocrine secretions with seizures in humans (Kleindienst et al., 2015; Wulsin et al., 2016). For example, abnormal plasma vasopressin levels resulted in hyponatremia due to the syndrome of inappropriate secretion of

antidiuretic hormone (SIADH) causing an increased intracranial pressure and seizures (Kleindienst et al., 2015).

The correlation between the neurohypophyseal volume with the mean latency to platform and mean path distance in Morris water-maze test for memory suggested that pituitary damage correlates with poor memory performance. A memory impairment is well documented in lateral FPI model of injury and is caused due to hippocampal atrophy and diffuse axonal injury of hippocampal network (Immonen et al., 2008).

MEMRI can serve as a good preclinical tool for investigating post-TBI structural changes when delivered in non-toxic concentrations (Silva et al., 2004). Future histologic studies are needed to specify the pathologies leading to pituitary atrophy in this experimental model of TBI. A recent study demonstrated safe use of FDA approved chelated manganese-based contrast agent, Teslascan, for MEMRI scan of brain and pituitary gland in adult volunteers opening doors for potential use of this method in identifying structural atrophies in hypophysis (Kim, 2015).

Overall, it can proposed that lobe-specific volumetric analysis of pituitary gland after TBI may serve as a surrogate marker of post-traumatic outcome and evolution of comorbidities. Further investigations will be, however, needed to evaluate whether the observed changes in neurohypophyseal volume and their correlations indicate causation or consequence of TBI-associated pathology and comorbidities.

7 CONCLUSIONS

The aim of this study was to characterize the spatiotemporal expression of SRPX2 protein in normal brain, to determine role of uPAR interactome in SRPX2 expression, and to identify TBI-induced changes in SRPX2 expression in brain and plasma. The main findings of this thesis can be summarized as follows:

1. SRPX2 is expressed in the hypothalamic Pa, Pe and SO nuclei of mouse, rat, monkey and human brain. SRPX2 protein is expressed in neurons and colocalizes with oxytocin or vasopressin in the Pa and SO nuclei. SRPX2 immunoreactive fibers project to the neurohypophysis and the brain stem. SRPX2 protein is present in rat and human plasma, as well as in human CSF.

2. SRPX2 expression in the hypothalamus is regulated independent of the uPAR interactome. CCI-induced TBI does not alter SRPX2 gene and protein expression in the hypothalamus. However, CCI-induced TBI differentially regulates uPAR and uPA gene expression in cortex, hippocampus and thalamus.

3. SRPX2 expression is acutely reduced in brain and plasma after lateral FPI-induced TBI. The reduction in SRPX2 plasma levels correlates with SRPX2 immunoreactivity in brain after a lateral FPI-induced TBI indicating SRPX2 as a candidate biomarker of hypothalamic injury.

4. Lateral FPI-induced TBI leads to chronic reduction in volume of neurohypophysis, which correlates with increased seizure susceptibility and poor spatial learning and memory.

Taken together, SRPX2 protein can serve as a novel target to modulate neuroendocrine and autonomic functions of the hypothalamo-pituitary axis in normal and injured brain. This thesis present basis for further investigations on injury-specific expression of SRPX2 protein and TBI-induced hypothalamic damage. It would be, however, essential to evaluate the translational capacity of these findings, and to investigate whether SRPX2 levels are differentially regulated after a TBI in humans. Moreover, it is still to be identified whether SRPX2 expression is associated with post-traumatic epilepsy, and if it can serve as a prognostic marker of epileptogenesis. Finally, mechanistic studies are needed to investigate the physiological and pathological regulation of SRPX2 expression in brain, and to identify the factors governing its systemic release.

REFERENCES

Acosta S, Lavarino C, Paris R, Garcia I, de Torres C, Rodríguez E, Beleta H, Mora J (2009) Comprehensive characterization of neuroblastoma cell line subtypes reveals bilineage potential similar to neural crest stem cells. BMC Dev Biol 9:12.

Algattas H, Huang JH (2013) Traumatic Brain Injury pathophysiology and treatments: early, intermediate, and late phases post-injury. Int J Mol Sci 15:309–341.

Andrade P, Paananen T, Ciszek R, Lapinlampi N, Pitkänen A (2018) Algorithm for automatic detection of spontaneous seizures in rats with post-traumatic epilepsy. J Neurosci Methods 307:37–45.

Aoki I, Wu Y-JL, Silva AC, Lynch RM, Koretsky AP (2004) In vivo detection of neuroarchitecture in the rodent brain using manganese-enhanced MRI. Neuroimage 22:1046–1059.

Archinti M, Britto M, Eden G, Furlan F, Murphy R, Degryse B (2011) The urokinase receptor in the central nervous system. CNS Neurol Disord Drug Targets 10:271–294.

Armstrong J, Taylor G, Thomas H, Boddy A, Redfern C, Veal G (2007) Molecular targeting of retinoic acid metabolism in neuroblastoma: the role of the CYP26 inhibitor R116010 in vitro and in vivo. Br J Cancer 96:1675–1683.

Baumann CR, Bassetti CL, Valko PO, Haybaeck J, Keller M, Clark E, Stocker R, Tolnay M, Scammell TE (2009) Loss of hypocretin (orexin) neurons with traumatic brain injury. Ann Neurol 66:555–559.

Beschorner R, Schluesener HJ, Nguyen TD, Magdolen V, Luther T, Pedal I, Mattern R, Meyermann R, Schwab JM (2000) Lesion-associated accumulation of uPAR/CD87-expressing infiltrating granulocytes, activated microglial cells/macrophages and upregulation by endothelial cells following TBI and FCI in humans. Neuropathol Appl Neurobiol 26:522–527.

Biomarkers, EndpointS, and other Tools Resource B (2016) BEST (Biomarkers, EndpointS, and other Tools) Resource. FDA-NIH Biomark Work Gr Available at: http://www.ncbi.nlm.nih.gov/pubmed/27010052 [Accessed August 19, 2019].

Blümcke I, Aronica E, Miyata H, Sarnat HB, Thom M, Roessler K, Rydenhag B, Jehi L, Krsek P, Wiebe S, Spreafico R (2016) International recommendation for a comprehensive neuropathologic workup of epilepsy surgery brain tissue: A consensus Task Force report from the ILAE Commission on Diagnostic Methods. Epilepsia 57:348–358.

Bolkvadze T, Pitkänen A (2012a) Development of Post-Traumatic Epilepsy after Controlled Cortical Impact and Lateral Fluid-Percussion-Induced Brain Injury in the Mouse. J Neurotrauma 29:789–812.

Bolkvadze T, Pitkänen A (2012b) Development of post-traumatic epilepsy after controlled cortical impact and lateral fluid-percussion-induced brain injury in the

mouse. J Neurotrauma 29:789–812.
Bolkvadze T, Puhakka N, Pitkänen A (2016) Epileptogenesis after traumatic brain injury in Plaur-deficient mice. Epilepsy Behav 60:187–196.
Bolkvadze T, Rantala J, Puhakka N, Andrade P, Pitkänen A (2015) Epileptogenesis after traumatic brain injury in Plau-deficient mice. Epilepsy Behav 51:19–27.
Booij HA, Gaykema WDC, Kuijpers KAJ, Pouwels MJM, Den Hertog HM (2018) Pituitary dysfunction and association with fatigue in stroke and other acute brain injury.
Bruneau N, Szepetowski P (2011) The role of the urokinase receptor in epilepsy, in disorders of language, cognition, communication and behavior, and in the central nervous system. Curr Pharm Des 17:1914–1923.
Bugge TH, Flick MJ, Daugherty CC, Degen JL (1995) Plasminogen deficiency causes severe thrombosis but is compatible with development and reproduction. Genes Dev 9:794–807.
Capatina C, Paluzzi A, Mitchell R, Karavitaki N (2015) Diabetes Insipidus after Traumatic Brain Injury. J Clin Med 4:1448–1462.
Carmeliet P, Kieckens L, Schoonjans L, Ream B, Nuffelen A Van, Prendergast G, Cole M, Bronson R, Collen D, Mulligan RC (1993) Plasminogen Activator Inhibitor-1 Gene-deficient Mice. 92:2746–2755.
Caston-Balderrama AL, Cameron JL, Hoffman GE (1998) Immunocytochemical localization of fos in perfused nonhuman primate brain tissue: Fixation and antisera selection. J Histochem Cytochem 46:547–556.
Deng H, Jankovic J, Guo Y, Xie W, Le W (2005) Small interfering RNA targeting the PINK1 induces apoptosis in dopaminergic cells SH-SY5Y. Biochem Biophys Res Commun 337:1133–1138.
Dewan MC, Rattani A, Gupta S, Baticulon RE, Hung Y-C, Punchak M, Agrawal A, Adeleye AO, Shrime MG, Rubiano AM, Rosenfeld J V., Park KB (2018) Estimating the global incidence of traumatic brain injury. J Neurosurg:1–18.
Dorton A (2000) The Pituitary Gland: Embryology, Physiology, and Pathophysiology. Neonatal Netw 19:9–17.
Drexel M, Puhakka N, Kirchmair E, Hörtnagl H, Pitkänen A, Sperk G (2015) Expression of GABA receptor subunits in the hippocampus and thalamus after experimental traumatic brain injury. Neuropharmacology 88:122–133.
Dusick JR, Wang C, Cohan P, Swerdloff R, Kelly DF (2012) Pathophysiology of hypopituitarism in the setting of brain injury. Pituitary 15:2–9.
Eagleson KL, Bonnin A, Levitt P (2005) Region- and age-specific deficits in γ-aminobutyric acidergic neuron development in the telencephalon of theuPAR-/- mouse. J Comp Neurol 489:449–466.
Eden G, Archinti M, Furlan F, Murphy R, Degryse B (2011) The Urokinase Receptor Interactome. Curr Pharm Des 17:1874–1889.
Ferguson A V, Latchford KJ, Samson WK (2008) The paraventricular nucleus of the hypothalamus – a potential target for integrative treatment of autonomic

dysfunction. Expert Opin Ther Targets 12:717–727.
Ferrer I, Martinez A, Boluda S, Parchi P, Barrachina M (2008) Brain banks: Benefits, limitations and cautions concerning the use of post-mortem brain tissue for molecular studies. Cell Tissue Bank 9:181–194.
Gao Z, Zhang J, Bi M, Han X, Han Z, Wang H, Ou Y (2015) SRPX2 promotes cell migration and invasion via FAK dependent pathway in pancreatic cancer. Int J Clin Exp Pathol 8:4791–4798.
Gasco V, Prodam F, Pagano L, Grottoli S, Belcastro S, Marzullo P, Beccuti G, Ghigo E, Aimaretti G (2012) Hypopituitarism following brain injury: when does it occur and how best to test? Pituitary 15:20–24.
GM S, RL C, RL H (2013) The human language-associated gene SRPX2 regulates synapse formation and vocalization in mice. Science (80-) 342:987–991.
Greco T, Hovda D, Prins M (2013) The Effects of Repeat Traumatic Brain Injury on the Pituitary in Adolescent Rats. J Neurotrauma 30:1983–1990.
Grundy PL, Harbuz MS, Jessop DS, Lightman SL, Sharples PM (2001) The hypothalamo-pituitary-adrenal axis response to experimental traumatic brain injury. J Neurotrauma 18:1373–1381.
Guaraldi F, Grottoli S, Arvat E, Ghigo E (2015) Hypothalamic-Pituitary Autoimmunity and Traumatic Brain Injury. J Clin Med 4:1025–1035.
Hayward NM, Immonen R, Tuunanen PI, Ndode-Ekane XE, Gröhn O, Pitkänen A (2010) Association of Chronic Vascular Changes with Functional Outcome after Traumatic Brain Injury in Rats. J Neurotrauma 27:2203–2219.
Hayward NMEA, Tuunanen PI, Immonen R, Ndode-Ekane XE, Pitkänen A, Gröhn O (2011) Magnetic resonance imaging of regional hemodynamic and cerebrovascular recovery after lateral fluid-percussion brain injury in rats. J Cereb Blood Flow Metab 31:166–177.
He F, Wang H, Li Y, Liu W, Gao X, Chen D, Wang Q, Shi G (2019) SRPX2 knockdown inhibits cell proliferation and metastasis and promotes chemosensitivity in esophageal squamous cell carcinoma. Biomed Pharmacother 109:671–678.
Herman ST (2002) Epilepsy after brain insult: targeting epileptogenesis. Neurology 59:S21-6.
Hong X, Hong X, Zhao H, He C (2018) Knockdown of SRPX2 inhibits the proliferation, migration, and invasion of prostate cancer cells through the PI3K/Akt/mTOR signaling pathway. J Biochem Mol Toxicol:e22237.
Huusko N, Römer C, Ndode-Ekane XE, Lukasiuk K, Pitkänen A (2015) Loss of hippocampal interneurons and epileptogenesis: a comparison of two animal models of acquired epilepsy. Brain Struct Funct 220:153–191.
Immonen RJ, Kharatishvili I, Gröhn H, Pitkänen A, Gröhn OHJ (2008) Quantitative MRI predicts long-term structural and functional outcome after experimental traumatic brain injury. Neuroimage 45:1–9.
Iyer AM, Zurolo E, Boer K, Baayen JC, Giangaspero F, Arcella A, Di Gennaro GC, Esposito V, Spliet WGM, van Rijen PC, Troost D, Gorter JA, Aronica E (2010) Tissue

plasminogen activator and urokinase plasminogen activator in human epileptogenic pathologies. Neuroscience 167:929–945.
Jackson SJ, Hussey R, Jansen MA, Merrifield GD, Marshall I, Maclullich A, Yau JLW, Bast T (2011) Manganese-enhanced magnetic resonance imaging (MEMRI) of rat brain after systemic administration of MnCl 2 : Hippocampal signal enhancement without disruption of hippocampus-dependent behavior. Behav Brain Res 216:293–300.
Johnson VE, Meaney DF, cullen DK, Smith DH (2015) Animal models of traumatic brain injury. Handb Clin Neurol 127:115–128.
Karhunen H, Pitkänen A, Virtanen T, Gureviciene I, Pussinen R, Ylinen A, Sivenius J, Nissinen J, Jolkkonen J (2003) Long-term functional consequences of transient occlusion of the middle cerebral artery in rats:: A 1-year follow-up of the development of epileptogenesis and memory impairment in relation to sensorimotor deficits. Epilepsy Res 54:1–10.
Kasturi BS, Stein DG (2009) Traumatic Brain Injury Causes Long-Term Reduction in Serum Growth Hormone and Persistent Astrocytosis in the Cortico-Hypothalamo-Pituitary Axis of Adult Male Rats. J Neurotrauma 26:1315–1324.
Kharatishvili I, Nissinen JP, McIntosh TK, Pitkänen A (2006) A model of posttraumatic epilepsy induced by lateral fluid-percussion brain injury in rats. Neuroscience 140:685–697.
Kharatishvili I, Pitkanen A (2010) Posttraumatic epilepsy. Curr Opin Neurol 23:183–188.
Kim SY (2015) Diagnosis and treatment of hypopituitarism. Endocrinol Metab 30:443–455.
Klein P et al. (2017) Commonalities in epileptogenic processes from different acute brain insults: Do they translate? Epilepsia.
Kleindienst A, Hannon MJ, Buchfelder M, Verbalis JG (2015) Hyponatremia in Neurotrauma: The Role of Vasopressin. J Neurotrauma 33:615–624.
Kovalevich J, Langford D (2013) Considerations for the use of SH-SY5Y neuroblastoma cells in neurobiology. Methods Mol Biol 1078:9–21.
Kozera B, Rapacz M (2013) Reference genes in real-time PCR. J Appl Genet 54:391–406.
Kurosawa H, Goi K, Inukai T, Inaba T, Chang KS, Shinjyo T, Rakestraw KM, Naeve CW, Look a T (1999) Two candidate downstream target genes for E2A-HLF. Blood 93:321–332.
Lahtinen L, Huusko N, Myöhänen H, Lehtivarjo AK, Pellinen R, Turunen MP, Ylä-Herttuala S, Pirinen E, Pitkänen A (2009) Expression of urokinase-type plasminogen activator receptor is increased during epileptogenesis in the rat hippocampus. Neuroscience 163:316–328.
Lahtinen L, Lukasiuk K, Pitkänen A (2006a) Increased expression and activity of urokinase-type plasminogen activator during epileptogenesis. Eur J Neurosci 24:1935–1945.
Lahtinen L, Lukasiuk K, Pitkänen A (2006b) Increased expression and activity of urokinase-type plasminogen activator during epileptogenesis. Eur J Neurosci

24:1935–1945.
Lesca G et al. (2013) GRIN2A mutations in acquired epileptic aphasia and related childhood focal epilepsies and encephalopathies with speech and language dysfunction. Nat Genet 45:1061–1066.
Lewis DA, Campbell MJ, Morrison JH (1986) An immunohistochemical characterization of somatostatin-28 and somatostatin-281–12in monkey prefrontal cortex. J Comp Neurol 248:1–18.
Lin X, Chang W, Wang Y, Tian M, Yu Z (2017) SRPX2, an independent prognostic marker, promotes cell migration and invasion in hepatocellular carcinoma. Biomed Pharmacother 93:398–405.
Liu B, Zhang B, Wang T, Liang QC, Jing XR, Zheng J, Wang C, Meng Q, Wang L, Wang W, Guo H, You Y, Zhang H, Gao GD (2010) Increased expression of urokinase-type plasminogen activator receptor in the frontal cortex of patients with intractable frontal lobe epilepsy. J Neurosci Res 88:2747–2754.
Liu K, Fan J, Wu J (2017) Sushi repeat-containing protein X-linked 2 promotes angiogenesis through the urokinase-type plasminogen activator receptor dependent integrin $\alpha v\beta 3$/focal adhesion kinase pathways. Drug Discov Ther 11:212–217.
Liu KL, Wu J, Zhou Y, Fan JH (2015) Increased Sushi repeat-containing protein X-linked 2 is associated with progression of colorectal cancer. Med Oncol 32:99.
Loewen SP, Paterson AR, Loh SY, Rogers MF, Hindmarch CCT, Murphy D, Ferguson A V. (2017) Sex-specific differences in cardiovascular and metabolic hormones with integrated signalling in the paraventricular nucleus of the hypothalamus. Exp Physiol 00:1–7.
Maas AI, Stocchetti N, Bullock R (2008) Moderate and severe traumatic brain injury in adults. Lancet Neurol 7:728–741.
Maas AIR et al. (2017) Traumatic brain injury: integrated approaches to improve prevention, clinical care, and research. Lancet Neurol 16:987–1048.
MacDermot KD, Bonora E, Sykes N, Coupe A-M, Lai CSL, Vernes SC, Vargha-Khadem F, McKenzie F, Smith RL, Monaco AP, Fisher SE (2005) Identification of FOXP2 Truncation as a Novel Cause of Developmental Speech and Language Deficits. Am J Hum Genet 76:1074–1080.
Mähler M, Berar M, Feinstein R, Gallagher A, Illgen-Wilcke B, Pritchett-Corning K, Raspa M (2014) FELASA recommendations for the health monitoring of mouse, rat, hamster, guinea pig and rabbit colonies in breeding and experimental units. Lab Anim 48:178–192.
Maiya B, Newcombe V, Nortje J, Bradley P, Bernard F, Chatfield D, Outtrim J, Hutchinson P, Matta B, Antoun N, Menon D (2008) Magnetic resonance imaging changes in the pituitary gland following acute traumatic brain injury. Intensive Care Med 34:468–475.
Makulski DD, Taber KH, Chiou-Tan FY (2008) Neuroimaging in posttraumatic hypopituitarism. J Comput Assist Tomogr 32:324–328.

Masos T, Miskin R (1997) mRNAs encoding urokinase-type plasminogen activator and plasminogen activator inhibitor-1 are elevated in the mouse brain following kainate-mediated excitation. Mol Brain Res 47:157–169.

McIntosh TK, Vink R, Noble L, Yamakami I, Fernyak S, Soares H, Faden AL (1989a) Traumatic brain injury in the rat: Characterization of a lateral fluid-percussion model. Neuroscience 28:233–244.

McIntosh TK, Vink R, Noble L, Yamakami I, Fernyak S, Soares H, Faden AL (1989b) Traumatic brain injury in the rat: characterization of a lateral fluid-percussion model. Neuroscience 28:233–244.

Moghieb A, Northwest P (2015) Acute, Subacute and Chronic Biomarkers for CNS Injury. In: Biomarkers of Brain Injury and Neurological Disorders (Wang K, Zhang Z, Kobeissy F, eds), pp 134–153. CRC Press.

Ndode-Ekane XE, Hayward N, Gröhn O, Pitkänen A (2010) Vascular changes in epilepsy: functional consequences and association with network plasticity in pilocarpine-induced experimental epilepsy. Neuroscience 166:312–332.

Ndode-Ekane XE, Pitkänen A (2013) Urokinase-Type Plasminogen Activator Receptor Modulates Epileptogenesis in Mouse Model of Temporal Lobe Epilepsy. Mol Neurobiol 47:914–937.

Osier ND, Dixon CE (2016) The controlled cortical impact model: Applications, considerations for researchers, and future directions. Front Neurol 7.

Peterson TC, Maass WR, Anderson JR, Anderson GD, Hoane MR (2015) A behavioral and histological comparison of fluid percussion injury and controlled cortical impact injury to the rat sensorimotor cortex. Behav Brain Res 294:254–263.

Pfundmair M, Lamprecht F, von Wedemeyer FM, Frey D (2016) Your word is my command: Oxytocin facilitates the understanding of appeal in verbal communication. Psychoneuroendocrinology 73:63–66.

Pitkänen A, Immonen R (2014) Epilepsy Related to Traumatic Brain Injury. Neurotherapeutics 11:286–296.

Pitkänen A, Kemppainen S, Ndode-Ekane XE, Huusko N, Huttunen JK, Gröhn O, Immonen R, Sierra A, Bolkvadze T (2014a) Posttraumatic epilepsy - disease or comorbidity? Epilepsy Behav 38:19–24.

Pitkänen A, Ndode-Ekane X, Lapinlampi N, Puhakka N (2018) Epilepsy biomarkers – Toward etiology and pathology specificity. Neurobiol Dis.

Pitkänen A, Ndode-Ekane XE, Łukasiuk K, Wilczynski GM, Dityatev A, Walker MC, Chabrol E, Dedeurwaerdere S, Vazquez N, Powell EM (2014b) Neural ECM and epilepsy.

Powell EM, Campbell DB, Stanwood GD, Davis C, Noebels JL, Levitt P (2003) Genetic disruption of cortical interneuron development causes region- and GABA cell type-specific deficits, epilepsy, and behavioral dysfunction. J Neurosci 23:622–631.

Prabowo AS, van Scheppingen J, Iyer AM, Anink JJ, Spliet WGM, van Rijen PC, Meeteren AYNS, Aronica E (2015) Differential expression and clinical significance of three inflammation-related microRNAs in gangliogliomas. J

Neuroinflammation 12:97.
Preissner KT, Kanse SM, May AE (2000) Urokinase receptor: a molecular organizer in cellular communication. Curr Opin Cell Biol 12:621–628.
Quirico-Santos T, Nascimento Mello A, Casimiro Gomes A, de Carvalho LP, de Souza JM, Alves-Leon S (2013) Increased metalloprotease activity in the epileptogenic lesion—Lobectomy reduces metalloprotease activity and urokinase-type uPAR circulating levels. Brain Res 1538:172–181.
Rantala J, Kemppainen S, Ndode-Ekane XE, Lahtinen L, Bolkvadze T, Gurevicius K, Tanila H, Pitkänen A (2015) Urokinase-type plasminogen activator deficiency has little effect on seizure susceptibility and acquired epilepsy phenotype but reduces spontaneous exploration in mice. Epilepsy Behav 42:117–128.
Reifschneider K, Auble B, Rose S, Reifschneider K, Auble BA, Rose SR (2015) Update of Endocrine Dysfunction following Pediatric Traumatic Brain Injury. J Clin Med 4:1536–1560.
Richmond E, Rogol AD (2014) Traumatic brain injury: endocrine consequences in children and adults. Endocrine 45:3–8.
Roe SY, McGowan EM, Rothwell NJ (1998) Evidence for the involvement of corticotrophin-releasing hormone in the pathogenesis of traumatic brain injury. Eur J Neurosci 10:553–559.
Roll P et al. (2006) SRPX2 mutations in disorders of language cortex and cognition. Hum Mol Genet 15:1195–1207.
Roll P, Vernes SC, Bruneau N, Cillario J, Ponsole-Lenfant M, Massacrier A, Rudolf G, Khalife M, Hirsch E, Fisher SE, Szepetowski P (2010) Molecular networks implicated in speech-related disorders: FOXP2 regulates the SRPX2/uPAR complex. Hum Mol Genet 19:4848–4860.
Rosenfeld J V, Maas AI, Bragge P, Morganti-Kossmann MC, Manley GT, Gruen RL (2012) Early management of severe traumatic brain injury. Lancet 380:1088–1098.
Royer-Zemmour B, Ponsole-Lenfant M, Gara H, Roll P, Lévêque C, Massacrier A, Ferracci G, Cillario J, Robaglia-Schlupp A, Vincentelli R, Cau P, Szepetowski P (2008a) Epileptic and developmental disorders of the speech cortex: ligand/receptor interaction of wild-type and mutant SRPX2 with the plasminogen activator receptor uPAR. Hum Mol Genet 17:3617–3630.
Royer-Zemmour B, Ponsole-Lenfant M, Gara H, Roll P, Lévêque C, Massacrier A, Ferracci G, Cillario J, Robaglia-Schlupp A, Vincentelli R, Cau P, Szepetowski P (2008b) Epileptic and developmental disorders of the speech cortex: ligand/receptor interaction of wild-type and mutant SRPX2 with the plasminogen activator receptor uPAR. Hum Mol Genet 17:3617–3630.
Royer-Zemmour B, Roll P, Cau P, Szepetowski P (2010) Epilepsy and the speech areas: identification and analysis of the interaction of the sushi-repeat protein SRPX2 with the plasminogen activator receptor uPAR. EPILEPSIES 22:14–17.
Royer B, Soares DC, Barlow PN, Bontrop RE, Roll P, Robaglia-Schlupp AA, Blancher A, Levasseur A, Cau P, Pontarotti P, Szepetowski P (2007) Molecular evolution of the

human SRPX2 gene that causes brain disorders of the Rolandic and Sylvian speech areas. BMC Genet 8:72.
Russell AL, Richardson MR, Bauman BM, Hernandez IM, Saperstein S, Handa RJ, Wu TJ (2018) Differential Responses of the HPA Axis to Mild Blast Traumatic Brain Injury in Male and Female Mice. Endocrinology 159:2363–2375.
Salmi M et al. (2013) Tubacin prevents neuronal migration defects and epileptic activity caused by rat Srpx2 silencing in utero. Brain 136:2457–2473.
Schirwani S, McConnell V, Willoughby J, Balasubramanian M (2019) Exploring the association between SRPX2 variants and neurodevelopment: How causal is it? Gene 685:50–54.
Semina E, Rubina K, Sysoeva V, Rysenkova K, Klimovich P, Plekhanova O, Tkachuk V (2016) Urokinase and urokinase receptor participate in regulation of neuronal migration, axon growth and branching. Eur J Cell Biol 95:295–310.
Sia GM, Clem RL, Huganir RL (2013) The human language-associated gene SRPX2 regulates synapse formation and vocalization in mice. Science 342:987–991.
Silva AC, Lee JH, Aoki I, Koretsky AP (2004) Manganese-enhanced magnetic resonance imaging (MEMRI): methodological and practical considerations. NMR Biomed NMR Biomed 17:532–543.
Skopin MD, Kabadi S V., Viechweg SS, Mong JA, Faden AI (2015) Chronic Decrease in Wakefulness and Disruption of Sleep-Wake Behavior after Experimental Traumatic Brain Injury. J Neurotrauma 32:289–296.
Smith DH, Soares HD, Pierce JS, Perlman KG, Saatman KE, Meaney DF, Dixon CE, McIntosh TK (1995) A Model of Parasagittal Controlled Cortical Impact in the Mouse: Cognitive and Histopathologic Effects. J Neurotrauma 12:169–178.
Smith HW, Marshall CJ (2010) Regulation of cell signalling by uPAR. Nat Rev Mol Cell Biol 11:23–36.
Soleman S, Filippov MA, Dityatev A, Fawcett JW (2013) Targeting the neural extracellular matrix in neurological disorders. Neuroscience 253:194–213.
Sumi Y, Dent MA, Owen DE, Seeley PJ, Morris RJ (1992) The expression of tissue and urokinase-type plasminogen activators in neural development suggests different modes of proteolytic involvement in neuronal growth. Development 116:625–637.
Sutiwisesak R, Kitiyanant N, Kotchabhakdi N, Felsenfeld G, Andrews PW, Wongtrakoongate P (2014) Induced pluripotency enables differentiation of human nullipotent embryonal carcinoma cells N2102Ep. Biochim Biophys Acta - Mol Cell Res 1843:2611–2619.
Swanson LW, Sawchenko PE (1983) Hypothalamic Integration: Organization of the Paraventricular and Supraoptic Nuclei. Annu Rev Neurosci 6:269–324.
Szmydynger-Chodobska J, Zink BJ, Chodobski A (2011) Multiple sites of vasopressin synthesis in the injured brain. J Cereb Blood Flow Metab 31:47–51.
Tanaka K, Arao T, Maegawa M, Matsumoto K, Kaneda H, Kudo K, Fujita Y, Yokote H, Yanagihara K, Yamada Y, Okamoto I, Nakagawa K, Nishio K (2009) SRPX2 is overexpressed in gastric cancer and promotes cellular migration and adhesion. Int

J Cancer 124:1072–1080.
Tanaka K, Arao T, Tamura D, Aomatsu K, Furuta K, Matsumoto K, Kaneda H, Kudo K, Fujita Y, Kimura H, Yanagihara K, Yamada Y, Okamoto I, Nakagawa K, Nishio K (2012) SRPX2 is a novel chondroitin sulfate proteoglycan that is overexpressed in gastrointestinal cancer. PLoS One 7:e27922.
Tang H, Zhao J, Zhang L, Zhao J, Zhuang Y, Liang P (2016) SRPX2 Enhances the Epithelial–Mesenchymal Transition and Temozolomide Resistance in Glioblastoma Cells. Cell Mol Neurobiol 36:1067–1076.
Tanriverdi F, Schneider HJ, Aimaretti G, Masel BE, Casanueva FF, Kelestimur F (2015) Pituitary dysfunction after traumatic brain injury: a clinical and pathophysiological approach. Endocr Rev 36:305–342.
Taylor SC, Berkelman T, Yadav G, Hammond M (2013) A defined methodology for reliable quantification of western blot data. Mol Biotechnol 55:217–226.
Teasdale G, Jennett B (1974) Assessment of coma and impaired consciousness. A Practical Scale. Lancet 304:81–84.
Theofanopoulou C, Boeckx C, Jarvis ED (2017) A hypothesis on a role of oxytocin in the social mechanisms of speech and vocal learning. Proc R Soc B Biol Sci 284:20170988.
Theunissen E, Baeten K, Vanormelingen L, Lambrichts I, Beuls E, Gelan J, Adriaensens P (2010) Detailed Visualization of the Functional Regions of the Rat Pituitary Gland by High-Resolution T2-Weighted MRI. J Vet Med Ser C Anat Histol Embryol 39:194–200.
Thompson HJ, Hoover RC, Tkacs NC, Saatman KE, Mcintosh TK (2005a) Development of posttraumatic hyperthermia after traumatic brain injury in rats is associated with increased periventricular inflammation. J Cereb Blood Flow Metab 25:163–176.
Thompson HJ, Lifshitz J, Marklund N, Grady MS, Graham DI, Hovda DA, McIntosh TK (2005b) Lateral Fluid Percussion Brain Injury: A 15-Year Review and Evaluation. J Neurotrauma 22:42–75.
Trabzuni D, Ramasamy A, Imran S, Walker R, Smith C, Weale ME, Hardy J, Ryten M, North American Brain Expression Consortium NABE (2013) Widespread sex differences in gene expression and splicing in the adult human brain. Nat Commun 4:2771.
Uhlen M, Bandrowski A, Carr S, Edwards A, Ellenberg J, Lundberg E, Rimm DL, Rodriguez H, Hiltke T, Snyder M, Yamamoto T (2016) A proposal for validation of antibodies. Nat Methods 13:823–827.
Undén L, Calcagnile O, Undén J, Reinstrup P, Bazarian J (2015) Validation of the Scandinavian guidelines for initial management of minimal, mild and moderate traumatic brain injury in adults. BMC Med 13.
Wei J, Xiao GM (2013) The neuroprotective effects of progesterone on traumatic brain injury: Current status and future prospects. Acta Pharmacol Sin 34:1485–1490.
West MJ, Slomianka L, Gundersen HJ (1991) Unbiased stereological estimation of the total number of neurons in thesubdivisions of the rat hippocampus using the

optical fractionator. Anat Rec 231:482–497.
Winslow JT, Hearn EF, Ferguson J, Young LJ, Matzuk MM, Insel TR (2000) Infant Vocalization, Adult Aggression, and Fear Behavior of an Oxytocin Null Mutant Mouse. Horm Behav 37:145–155.
Wulsin AC, Solomon MB, Privitera MD, Danzer SC, Herman JP (2016) Hypothalamic-pituitary-adrenocortical axis dysfunction in epilepsy. Physiol Behav 166:22–31.
Xiong Y, Mahmood A, Chopp M (2013) Animal models of traumatic brain injury. Nat Rev Neurosci 14:128–142.
Yamada T, Oshima T, Yoshihara K, Sato T, Nozaki A, Shiozawa M, Ota M, Yoshikawa T, Akaike M, Numata K, Rino Y, Kunisaki C, Tanaka K, Imada T, Masuda M (2014) Impact of overexpression of Sushi repeat-containing protein X-linked 2 gene on outcomes of gastric cancer. J Surg Oncol 109:836–840.
Ye Z, Stolk A, Toni I, Hagoort P (2016) Oxytocin Modulates Semantic Integration in Speech Comprehension. J Cogn Neurosci 29:1–10.
Yehuda R (2001) Biology of posttraumatic stress disorder. J Clin Psychiatry 62 Suppl 17:41–46.
Yuan XQ, Wade CE (1991) Neuroendocrine abnormalities in patients with traumatic brain injury. Front Neuroendocrinol 12:209–230.
Zhang HF, Dai YC, Wu J, Jia MX, Zhang JS, Shou XJ, Han SP, Zhang R, Han JS (2016) Plasma Oxytocin and Arginine-Vasopressin Levels in Children with Autism Spectrum Disorder in China: Associations with Symptoms. Neurosci Bull 32:423–432.
Zhou Y (2017) Abnormal structural and functional hypothalamic connectivity in mild traumatic brain injury. J Magn Reson Imaging 45:1105–1112.

APPENDICES

APPENDIX 1.

MEHWISH ANWER

Traumatic brain injury (TBI) leads to neurobiological and psychological abnormalities in millions of people each year, globally. This thesis explores the expression of Sushi repeat-containing protein X-linked 2 (SRPX2), in brain, and the effect of TBI on SRPX2 expression in brain and SRPX2 protein levels in blood. The study identified SRPX2 as a novel biomarker of TBI.

UNIVERSITY OF
EASTERN FINLAND

uef.fi

**PUBLICATIONS OF
THE UNIVERSITY OF EASTERN FINLAND**
Dissertations in Health Sciences

ISBN 978-952-61-3324-9
ISSN 1798-5706